The Journal of Immunology



# Disruption of the Transcription Factor Nrf2 Promotes Pro-Oxidative Dendritic Cells That Stimulate Th2-Like Immunoresponsiveness upon Activation by Ambient Particulate Matter

Marc A. Williams, Tirumalai Rangasamy, Stephen M. Bauer, Smruti Killedar, Matthew Karp, Thomas W. Kensler, Masayuki Yamamoto, Patrick Breysse, Shyam Biswal and Steve N. Georas

*J Immunol* 2008; 181:4545-4559; ;
doi: 10.4049/jimmunol.181.7.4545
http://www.jimmunol.org/content/181/7/4545



*The Journal of Immunology* is published twice each month by
The American Association of Immunologists, Inc.,
1451 Rockville Pike, Suite 650, Rockville, MD 20852

Print ISSN: 0022-1767 Online ISSN: 1550-6606.

# Disruption of the Transcription Factor Nrf2 Promotes Pro-Oxidative Dendritic Cells That Stimulate Th2-Like Immunoresponsiveness upon Activation by Ambient Particulate Matter[1]

**Marc A. Williams,[2,3]*† Tirumalai Rangasamy,[2]* Stephen M. Bauer,* Smruti Killedar,* Matthew Karp,* Thomas W. Kensler,‡ Masayuki Yamamoto,¶ Patrick Breysse,‡ Shyam Biswal,‡§ and Steve N. Georas[3]*†**

**Oxidative stress is important in dendritic cell (DC) activation. Environmental particulate matter (PM) directs pro-oxidant activities that may alter DC function. Nuclear erythroid 2 p45-related factor 2 (*Nrf2*) is a redox-sensitive transcription factor that regulates expression of antioxidant and detoxification genes. Oxidative stress and defective antioxidant responses may contribute to the exacerbations of asthma. We hypothesized that PM would impart differential responses by *Nrf2* wild-type DCs as compared with Nrf2$^{-/-}$ DCs. We found that the deletion of *Nrf2* affected important constitutive functions of both bone marrow-derived and highly purified myeloid lung DCs such as the secretion of inflammatory cytokines and their ability to take up exogenous Ag. Stimulation of *Nrf2*$^{-/-}$ DCs with PM augmented oxidative stress and cytokine production as compared with resting or *Nrf2*$^{+/+}$ DCs. This was associated with the enhanced induction of *Nrf2*-regulated antioxidant genes. In contrast to *Nrf2*$^{+/+}$ DCs, coincubation of *Nrf2*$^{-/-}$ DCs with PM and the antioxidant *N*-acetyl cysteine attenuated PM-induced up-regulation of CD80 and CD86. Our studies indicate a previously underappreciated role of *Nrf2* in innate immunity and suggest that deficiency in *Nrf2*-dependent pathways may be involved in susceptibility to the adverse health effects of air pollution in part by promoting Th2 cytokine responses in the absence of functional *Nrf2*. Moreover, our studies have uncovered a hierarchal response to oxidative stress in terms of costimulatory molecule expression and cytokine secretion in DCs and suggest an important role of heightened oxidative stress in proallergic Th2-mediated immune responses orchestrated by DCs.** *The Journal of Immunology,* **2008, 181: 4545–4559.**

A major public health concern is the global increase in urban and roadside traffic pollution. Despite its importance, there is poor appreciation and understanding of how exposure to particulates contained in environmental airborne pollution affect the immune system. Although there is currently a lack of data indicating the mechanisms involved, some studies have suggested that inhaled particulate matter (PM)[4] derived from industry, power stations, or diesel exhaust particles contribute to the increased incidence of asthma, allergic conditions, pulmonary infections, cardiovascular disease, and mortality in the infant and adult populations (1–5). In addition, different types of air pollution can have profoundly different qualitative effects on human health (3).

Dendritic cells (DCs) are the key components of innate immunity that rapidly responds to diverse environmental cues. Because DCs are highly efficient in activating naive T cells, they link innate and adaptive immunity during episodes of infection or cellular damage and tissue necrosis. In this way, DCs efficiently activate naive T cells, resulting in their clonal expansion and differentiation into different effector lineages (6–9). Although DCs are poised to

*Division of Pulmonary and Critical Care Medicine and †Department of Environmental Medicine, University of Rochester School of Medicine and Dentistry, Rochester, NY 14642; ‡Department of Environmental Health Sciences, Johns Hopkins Bloomberg School of Public Health, and §Division of Pulmonary and Critical Care Medicine, Johns Hopkins University School of Medicine, Baltimore, MD 21205; and ¶Center for Tsukuba Advanced Research Alliance, University of Tsukuba, Tsukuba, Japan

Received for publication June 29, 2007. Accepted for publication July 23, 2008.

The costs of publication of this article were defrayed in part by the payment of page charges. This article must therefore be hereby marked *advertisement* in accordance with 18 U.S.C. Section 1734 solely to indicate this fact.

[1] This research was supported in part by a New Investigator Project from the Center for Childhood Asthma in the Urban Environment (funded by National Institute of Environmental Health Sciences (NIEHS) and U.S. Environmental Protection Agency Grant P01ES09606 to S.N.G. and M.A.W.) as well as by the Department of Medicine, University of Rochester School of Medicine and Dentistry (Rochester, NY). The research was also supported by National Institutes of Health (NIH) Research Grants R01 HL073952 and HL071933 (to S.N.G.), COPD SCCOR P50 HL084945 and CA 94076 (to T.W.K.) and by NIH NIEHS Pilot Project Grants P30 ES03819 and P30 ES001247 (to M.A.W.).

M.A.W. wrote the paper, performed the research, analyzed the data, and was responsible for the design and implementation of the experiments. T.R. cowrote the paper, performed the research with M.A.W., and assisted with the analysis of the data as well as with the design and implementation of the experiments. S.K. assisted with the technical aspects of the experiments and also contributed important elements for the design and implementation of some of the experiments. M.K. provided important technical assistance and data analysis in the execution of some of the experimental assays. S.M.B. assisted with the design and implementation of the data derived from lung DCs and naive CD4$^+$ T cell coculture studies as well as with the measurement of cytokine production. T.W.K. provided vital new reagents and analytical tools and assisted with analysis of some of the data. M.Y. contributed vital materials to this study. P.B. contributed vital materials to this study as well as methodological approaches in using particulate matter. S.B. assisted in the experimental design and data analysis. S.N.G. assisted in the experimental design, critical discussion, and data analysis.

[2] M.A.W. and T.R. contributed equally to this work.

[3] Address correspondence and reprint requests to Dr. Marc. A. Williams or Dr. Steve N. Georas, Division of Pulmonary and Critical Care Medicine, University of Rochester School of Medicine, 601 Elmwood Avenue, Box 692, Rochester, NY 14642-8692. E-mail addresses: marc_williams@urmc.rochester.edu or steve_georas@urmc.rochester.edu

[4] Abbreviations used in this paper: PM, particulate matter; APM, ambient particulate matter; CD40L, CD40 ligand; DC, dendritic cell; DCF, dichlorofluorescein; DCFH-DA, 2′,7′-dichlorofluorescein diacetate; DX, dextran; GCLc, glutathione cysteine ligase catalytic subunit; GCLm, GCLc modifier subunit; HO-1, hemeoxygenase-1; KC, keratinocyte; MFI, mean fluorescence intensity; NAC, *N*-acetyl cysteine; Nrf2, nuclear erythroid 2 p45-related factor 2; PDCA-1, plasmacytoid DC Ag-1; ROS, reactive oxygen species; VEGF, vascular endothelial growth factor; wt, wild type.

respond to inhaled pollutants such as ambient particulate matter (APM), very little is known about how APM affects the activation of DCs. Interestingly, other groups have recently reported that human airway epithelial cells exposed to diesel exhaust particles secrete chemokines and other mediators that recruit DCs and induce their maturation (10, 11). Thus, DCs will be among the first cells to sense and respond to inhaled particulate pollution.

Airway inflammation in allergic asthma reflects aberrant immune responses against otherwise harmless inhaled allergens (9). Although DCs reside in the airway and are richly interdigitated throughout the bronchial epithelium (12), little is known about how inhaled environmental exposures affect DCs. We have previously shown that ambient urban PM instructs a novel pathway of DC maturation and directs them to stimulate a complex pattern of Th1- and Th2-associated T cell responses (2). Oxidative stress is important in DC maturation and could influence the ultimate pattern of immune responses (13, 14). DCs also require a balanced intracellular redox state for proper functional development (15–19). Depletion of glutathione in murine APCs in vivo resulted in suppressed Th1 and elevated Th2 activity (19). Oxidative stress occurs when oxidants overwhelm antioxidant defenses that may also involve signaling via the transcription factor NFκB under conditions of accumulated hydrogen peroxide (20). To counteract the deleterious effects of oxidative stress, all cells have evolved an elaborate defense mechanism to maintain redox homeostasis. This system includes a series of antioxidant detoxification enzymes (21–26).

The nuclear erythroid 2 p45-related factor 2 (*Nrf2*) has been shown by our group and others to be a key regulatory transcription factor that induces antioxidant and detoxification genes that protect against the deleterious effects of reactive oxygen species (ROS) (22–27). *Nrf2* is a redox-sensitive, basic leucine zipper transcription factor. During oxidative stress, *Nrf2* is activated following its detachment from a cytosolic inhibitor called Keap1 and then translocates to the nucleus where it binds to the antioxidant response element in the promoter region of target genes, leading to their transcriptional induction (22–28).

We have shown that genetic deletion of *Nrf2* renders mice more susceptible to Th2-driven allergic airway inflammation (25). This suggested that *Nrf2* normally functions to maintain allergen-driven immune responses in check. However, the mechanisms of how *Nrf2* regulates immune responses and responds to diverse environmental danger signals remains poorly understood. Clues to the potential importance of *Nrf2* in host immunity come from studies in *Nrf2*-deficient mice (29). These mice were more susceptible to sepsis in part due to the augmented transcription of several innate immune response genes (29). This study suggested that *Nrf2* may be important in regulating innate immunity. Interestingly, Li and colleagues showed that *Nrf2* is activated by diesel exhaust particles in epithelial cells and macrophages (22, 23), but how *Nrf2* function in dendritic cells remains poorly understood.

In the present study, we exposed bone marrow-derived DCs from $Nrf2^{+/+}$ and $Nrf2^{-/-}$ mice to urban airborne PM to assess whether a defective antioxidant defense in DCs would alter their responses to an important environmental airborne pollutant. Disruption of *Nrf2* in DCs leads to increased oxidative stress and a dysregulated pattern of immunological responsiveness in PM-exposed DCs that was also characterized by an enhanced promotion of a Th2-type immune response upon the coculture of APM-stimulated $Nrf2^{-/-}$ lung DCs with naive $CD4^+$ OT-II T cells. These studies point to a crucial role for Nrf2 in innate immunity and oxidative defense mechanisms in response to airborne particulate pollution.

## Materials and Methods

### *Use of wild-type (wt) and Nrf2 gene-disrupted mice*

*Nrf2*-deficient CD1:ICR mice were generated as previously described (30). Mice were genotyped for *Nrf2* expression by PCR amplification of genomic DNA extracted from the tail using three different primers (19) as follows: 5′-TGGACGGGACTATTGAAGGCTG-3′ (sense for both genotypes); 5′-CGCCTTTTCAGTAGATGGAGG-3′ (antisense for wt *Nrf2* mice); and 5′-GCGGATTGACCGTAATGGGATAGG-3′ (antisense for LacZ). All investigations done with mice met the approval of the Johns Hopkins University Animal Care and Use Committee and were conducted in strict accordance with guidelines set by the U.S. Animal Welfare Acts and National Institutes of Health guidelines. Male OT-II transgenic mice expressing the TCR specific for OVA323–339 were also used in this study (see below) and maintained in the laboratory animal research facility of the University of Rochester (Rochester, NY) concordant with the approval of the University of Rochester Animal Care and Use Committee. Both strains of mice were propagated in specific pathogen-free conditions, fed an AIN-76A diet and water ad libitum, and housed in polycarbonate cages with hard wood chip bedding in a conventional animal facility maintained under controlled conditions (temperature at 23 ± 2°C, humidity of 55 ± 5%, and continuous light/dark cycles of 12 h).

### *Generation of murine DCs and stimulation*

Myeloid DCs were generated from bone marrow-derived precursors of naive $Nrf2^{+/+}$ and $Nrf2^{-/-}$ mice as described using a highly reproducible protocol that generates conventional myeloid DC (online supplemental material for Ref. 2) in static culture at 37°C in a fully humidified 5% $CO_2$/95% air incubator. Bone marrow precursors were harvested from the pooled femurs and tibiae of female mice (8 wk old; five mice per genotype per independent experiment) by flushing with ice-cold complete RPMI 1640 culture medium (Dutch modification) supplemented with 20 mM HEPES buffer, 2 mM L-glutamine, 2.5 μg/ml gentamicin sulfate, and 8% (v/v) FBS; aggregates were gently disbursed by repeated pipetting in ice-cold culture medium. Cells were centrifuged at 400 × *g* for 10 min at 8°C and, following two washes in ice-cold divalent cation-free PBS (pH 7.4), the cells were resuspended and the erythrocytes were removed by lysis in ACK buffer (150 mM $NH_4Cl$, 1.0 mM $KHCO_3$, and 0.1 mM $Na_2EDTA$ (pH 7.4)) for 3 min at room temperature. The lysis reaction was quenched by the addition of ice-cold culture medium and centrifugation at 400 × *g* for 10 min at 8°C. Cells were resuspended in PBS containing 10 mM EDTA, 0.1% BSA, and 10 mM HEPES, and centrifuged twice at 200 × *g* for 10 min at 8°C to deplete platelets (we have found that platelets can adversely block the development of conventional myeloid DC and reduce the yield; thus, we prefer to remove them). Cell pellets were next resuspended in culture medium and seeded into 6-well tissue culture clusters at a density of $2.5 \times 10^5$ cells per well in a total volume of 4 ml. Cells were cultured at 37°C in a sterile filtered atmosphere of 5% $CO_2$/95% air and a fully humidified incubator. Cultures were pulsed at day 0 and every 48 h with a combination of IL-4 (10 ng/ml) and GM-CSF (25 ng/ml) to propagate immature myeloid DC as we have previously described (2). After 8 days of culture, immature DCs were harvested, washed, and seeded at a density of $8 \times 10^5$ cells/ml in 12-well culture dishes in a total volume of 2.0 ml. Immature DCs propagated by this method were conventional myeloid DCs with an end of culture viability of at least 95.6 ± 2.9% (by 0.2% (v/v) trypan blue exclusion and light microscopic evaluation). Immature myeloid DCs were characterized as moderate expressing $CD11c^+$, high expressing $CD11b^+$, and moderate expressing MHC class II (Ia/Ie haplotype) cells, as described in Fig. 1. Immature DCs were next stimulated with culture medium alone (resting immature DC), 100 ng/ml LPS (*Escherichia coli*-derived endotoxin, serotype 055:B5, in endotoxin-free water), or 10 μg/ml Baltimore city ambient particulate matter ($PM_{10}$) in endotoxin-free PBS with 20 mM HEPES buffer (pH 7.4). In some experiments, carbon black particles were used as a negative control to test for any PM-mediated, contact-dependent activation of DCs at 10 μg/ml (Sigma-Aldrich). Following 48 h of culture, we harvested DCs and culture supernatant to assess cell function and secretion of cytokines.

### *Isolation and purification of conventional myeloid lung DCs*

In some experiments, we confirmed our observations made with bone marrow-derived DC from $Nrf2^{+/+}$ as compared with $Nrf2^{-/-}$ by studying the functional and activation-dependent responses of CD11c-selected conventional myeloid lung DC using a protocol developed in our laboratory. In three independent experiments, we enriched for pulmonary myeloid $CD11c^+$PDCA-$1^-$ DC (Fig. 1; where PDCA is plasmacytoid DC Ag-1). Although we have reproducibly applied this protocol in our laboratory, it

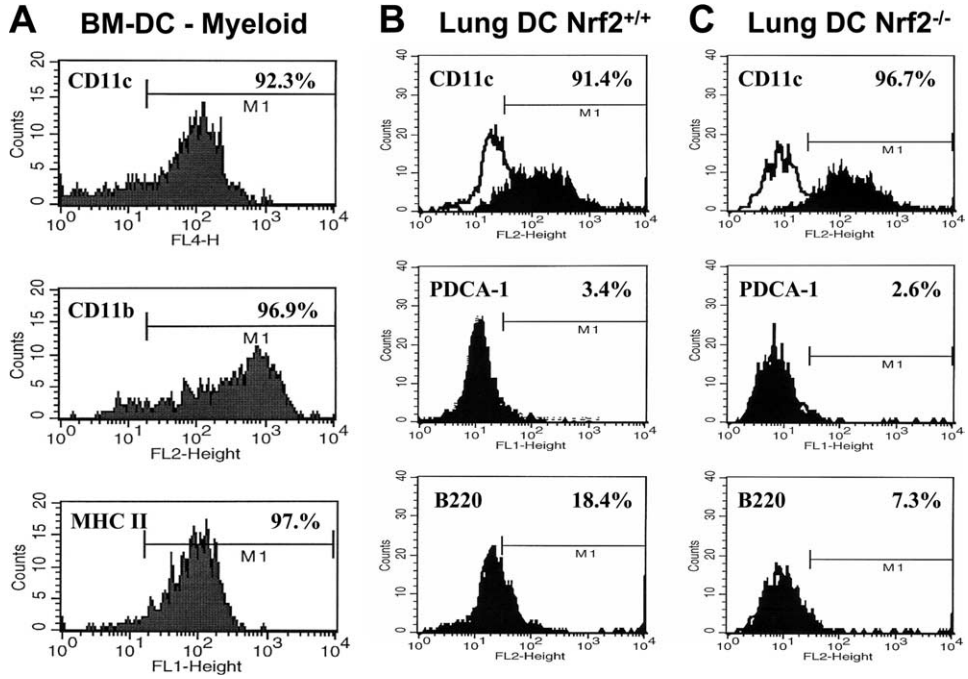


**FIGURE 1.** Determination of the cell surface markers that characterize bone marrow-derived DCs (BM-DC) in liquid static culture (*A*) for the experiments described herein and the highly purified rare myeloid conventional DCs subpopulation enriched from the pooled lungs of $Nrf2^{+/+}$ (*B*) and $Nrf2^{-/-}$ (*C*) mice. Cell surface expressions, shown here as flow cytofluorographic histograms, were typical of several enrichments conducted in our laboratory and were determined by real-time flow cytometry (FACScalibur and CellQuest software). For bone-marrow-derived DCs, the myeloid DC phenotype (*A*) was confirmed by high expression of an CD11c-allophycocyanin conjugate and coexpression of CD11b-PE, with low-moderate expression of MHC class II-FITC typical of resting state immature DCs. For purified lung DCs, the myeloid DC phenotype was confirmed by expression of CD11c-PE, absence of the plasmacytoid DC marker PDCA-1-FITC, and low to very low expression of B220-PE in both $Nrf2^{+/+}$ DCs and $Nrf2^{-/-}$ DCs. Data are described as MFI.

has not been previously published by us; for that reason, it is described in full in this article.

Groups of four to five mice per genotype were euthanized one at a time by i.p. injection of 200 mg/kg sodium pentobarbital euthanasia solution, and then cervical dislocation, consistent with University of Rochester Institutional Animal Care and Use Committee protocols and the most recent guidelines on euthanasia from the American Veterinary Medical Association. Upon confirmation of euthanasia, the abdominal aorta was severed and immediately blotted with sterile surgical gauze, and the diaphragm as well as the rib cage was then excised. Next, the right and left ventricles of the heart were perfused with two successive 5.0-ml volumes of ice-cold PBS (divalent cation-free) supplemented with 20 IU/ml sodium heparin. Next, the heart was clamped and excised after the removal of pericardiac membrane. Using forceps, the trachea was grasped and cut close to the head of animal so that the lungs and trachea could be removed from the mouse. The trachea was then resected, leaving ~2–4 mm above the lungs for manipulation of the organs. Up to five whole lungs were deposited into 20 ml of digest buffer (divalent cation-free PBS, 10 mM HEPES-NaOH (pH 7.4) supplemented with 150 mM NaCl, 5 mM KCl, 1 mM $MgCl_2$, and 1.8 mM $CaCl_2$) on ice and, using a 10-$cm^2$ petri culture-dish, the lungs were sliced into fragments of ~2-$mm^2$ using two sterile scalpel blades. The culture dish was washed with an additional 5 ml of digest buffer to collect residual lung fragments for a total volume of 25 ml. Just before incubation at 37°C in a standard cell culture incubator, the digest buffer was supplemented with tissue-digesting enzymes, including collagenase II (Worthington Laboratories) at 2.0 mg/ml, dispase II (Sigma-Aldrich) at 0.25 mg/ml, and DNase I (Sigma-Aldrich) at 2.0 mg/ml. The crude tissue homogenate was incubated for 30–45 min with periodic agitation by inverting the tube 8–10 times every 5 min. The suspension was then diluted with an equal volume of filter-sterilized GKN buffer (11 mM D-glucose, 5.5 mM KCl, 137 mM NaCl, 25 mM $Na_2HPO_4$, and 5.5 mM $NaH_2PO_4$) supplemented with 2 mM EDTA and 5% (v/v) FBS that was held at 37°C until use. Next, the digest was passed over a 70-$\mu$m nylon cell strainer to liberate a single cell suspension, which was washed twice with 10 ml of GKN plus 5% FBS; the washings were collected into the same tube, centrifuged at 450 × *g* for 10 min at 25°C, and the supernatant was discarded carefully. The cell pellet was resuspended in 10 ml of culture medium, and the contaminating $CD11c^+$ macrophages in this cell suspension were removed by adherence to tissue culture grade 10-$cm^2$ plastic dishes for 1 h at 37°C. The macrophage-depleted, cell-rich supernatant was harvested and centrifuged at 400 × *g* for 8 min at 20°C. The cell pellet was then carefully resuspended in ice-cold MACS cell separation buffer (divalent cation-free PBS supplemented with 2 mM EDTA and 2.5% (v/v) FBS) to 10 ml and centrifuged at 250 × *g* for 10 min at 8°C. Next, plasmacytoid DCs were removed by following the direct selection procedure for immunomagnetic isolation of PDCA-1-expressing plasmacytoid DCs (Miltenyi Biotech). The PDCA-1 depleted lung DCs were then subjected to the conventional myeloid CD11c DC direct enrichment procedure following the manufacturer's protocol (Miltenyi Biotec). Using the above protocol, from groups of four mice we routinely harvested $4.3 \times 10^5$ to $1.25 \times 10^6$ $CD11c^+$ DCs (90.8–97.6% pure by flow cytometric quantitation of CD11c expression) of purified DC. The low yield of highly purified lung DCs that one obtains using the above procedure relative to the vast numbers that one liberates from bone marrow precursors favors much of our work to be modeled using bone marrow-derived DCs and not lung DCs. Nonetheless, sufficient numbers are obtained that permit basic flow cytometric and cytokine secretion-type assays upon the activation of CD11c lung DCs as well as carefully designed naive allogeneic $CD4^+$ T cell/DC cocultures.

### *Baltimore city ambient particulate matter*

Ambient PM was collected in the spring of 2001 (April-June) using a high-volume cyclone collector with a theoretical cut point of 0.85-$\mu$m aerodynamic diameter as we have described in detail (2). Collected APM was pooled, stored under nitrogen gas, and then refrigerated until use. Before use, 10 mg/ml APM was suspended in 20 mM HEPES-buffered, divalent cation-free PBS (pH 7.4), vortexed at a high speed for 5 min, and used immediately. The toxicity of APM was tested against murine bone marrow-derived DCs by monitoring trypan blue exclusion. After 48 h of culture, the toxic dose of APM that induced 50% killing ($TD_{50}$) was <540 $\mu$g/ml. All experiments were done using APM at 10 $\mu$g/ml. We excluded the possibility that endotoxin contamination of APM may provoke DC activation by the *Limulus* amebocyte lysate QCL-1000 assay (Cambrex). We found contaminating levels to be <50 pg of endotoxin per 100 $\mu$g/ml APM. We have previously shown in detailed titration analyses against immature murine DC that the very low concentrations of endotoxin we

found to be present in atmospheric APM (<50 pg of endotoxin per 100 μg/ml APM) did not affect either the cell surface expression of activation markers or the secretion of inflammatory cytokines, nor did it alter significantly the interaction of DCs with naive $CD^+$ T cells (online supplemental material for Ref. 2). In these experiments, we investigated the dose-dependent effects of APM on DCs by reciprocal 10-fold dilutions and contrasted the observations against the equivalent levels of endotoxin found to be present in APM by reciprocal 10-fold dilutions (online supplemental material for Ref. 2).

### *Treatment with* N*-acetyl cysteine (NAC)*

To determine the effect of PM (Sigma-Aldrich) instructing DC activation by an oxidative stress-mediated mechanism, we cultured DCs as described and, on day 8, stimulated the DCs in the absence/presence of APM (10 μg/ml) with/without NAC (5 mM) for 48 h. DCs were analyzed by flow cytometry for cell surface markers or by ELISA for cytokine secretion. To maximize antioxidant activity, DCs were pretreated with NAC for 1 h before adding PM for the remaining 48-h incubation period.

### *Characterization of cell membrane-expressed maturation markers of DC*

We used multiparameter flow cytometry to measure the expression of function-associated molecules by bone marrow-derived as well as highly purified, freshly isolated myeloid lung DC as previously described (2). DCs were harvested 48 h after stimulation (as described above) and resuspended in divalent cation-free PBS supplemented with 2% (v/v) FCS and 0.2% (w/v) sodium azide (FACS buffer). DC preparations were blocked in 5% (v/v) normal mouse serum for 15 min at 4°C, washed twice in FACS buffer, and then secondarily blocked for 15 min at 4°C in anti-mouse CD16/CDw32 (mouse BD Fc block, clone 2.4G2; BD Pharmingen) to prevent nonspecific Fc-γ receptor-mediated binding of specific detection Abs. DC preparations were next stained immediately with the following FITC or PE fluorochrome-conjugated mAbs (BD Pharmingen): anti-MHC class II-PE or FITC (polymorphic Ia/Ie determinants), anti-CD11b-PE, anti-CD11c-PE, anti-CD80-PE, anti-CD86-PE, and anti-CD40-PE. In assays where the enrichment and purity of bone marrow-derived DCs and lung DCs required confirmation, we also used anti-CD45R/B220-PE (BD Pharmingen), anti-PDCA-1-FITC (clone JF05-1C2.4.1; Miltenyi Biotec), and anti-CD11c-allophycocyanin (clone N418; Miltenyi Biotec). Samples were washed twice in FACS buffer by centrifugation at 400 × *g* for 6 min at 4°C and fixed in 2% (v/v) paraformaldehyde in FACS buffer before analysis. We analyzed samples on a FACSCalibur flow cytometer using CellQuest 3.1 software (BD Biosciences). The instrument had a standard optical filter configuration with band pass filters of 530/30 nm and 585/44 nm for FL1 (FITC-conjugated antibodies) and FL2 (PE-conjugated antibodies) data acquisition, respectively. For the analysis of forward angle light scatter, side angle light scatter, and cell surface receptor expression, data were acquired in real time. Cell surface expression data were acquired in real time as geometric mean fluorescence intensity (MFI). The instrument was standardized before phenotypic analysis with calibration beads (FluoroSpheres 6-Peak; DakoCytomation) and cleaned with sequential washes of distilled water, 10% (v/v) hypochlorite, and distilled water before data acquisition.

### *Cytokine measurements*

Cell-free culture supernatants were enumerated for cytokine concentrations by commercial ELISA. We measured the secretion of IL-6 and IL-10 (both from E-Bioscience with a sensitivity of 2.5 pg/ml cytokine), IL-18 (from MBL International with a sensitivity of 12.5 pg/ml cytokine), and IL-12p40 and TNF-α (both from Invitrogen-BioSource with limits of sensitivity of 7.5 pg/ml cytokine). We also measured levels of vascular endothelial growth factor (VEGF)-A (R&D Systems). The VEGF ELISA possessed limits of sensitivity of 7.8 pg/ml. Cytokine secretion was measured in both bone marrow-derived DCs as well as the myeloid lung DCs purified from $Nrf2^{+/+}$ and $Nrf2^{-/-}$ mice. In $CD11c^+$ lung DCs, we measured the time-dependent secretion of TNF-α, IL-12p40, and keratinocyte-derived chemokine (KC/CXCL1) at 24, 48, and 72 h poststimulation with PM such that the duration and peak production of these inflammatory cytokines of PM-stimulated DC could be determined. We reported data as picograms of secreted product per $10^6$ DC. All measurements were done according to the manufacturer's guidelines.

### *Enrichment of highly pure naive $CD4^+$ T cells from OT-II mice*

Male OT-II transgenic mice expressing the TCR specific for OVA323–339 and MHC I-$A^b$ on the C57BL/6 genetic background were provided by Dr. D. Topham (University of Rochester School of Medicine, Rochester, NY). These mice were housed in dedicated pathogen-free facilities at the University of Rochester. For purposes of isolating and purifying naive $CD4^+$ T cells, pools of four mice were euthanized by $CO_2$ asphyxiation followed by cervical dislocation and removal of the superficial inguinal, lumbar, sacral, renal, axillary, brachial, and cervical nodes. A single mononuclear cell suspension in complete RPMI 1640 culture medium was prepared from the lymph nodes, which were next washed twice at 300 × *g* for 10 min at 4°C. After the final wash, cells were resuspended in 8 ml of ice-cold, serum-free culture medium and layered over a cushion of 5 ml of Lympholyte M at a density of 1.0875 g/$cm^3$ (pH 6.9) (Cedarlane). This is a density cell separation medium specifically optimized for the isolation of viable lymphocytes from murine lymphoid cell suspensions. This procedure depleted cell debris, fatty tissue, erythrocytes, platelets, and nonviable cells from the lymphocyte preparation. The interface lymphocytes were harvested and washed twice in ice-cold complete culture medium and once in MACS buffer (divalent cation-free PBS supplemented with 2.5% FBS and 2 mM EDTA) at 300 × *g* for 10 min at 4°C. Cells were then subjected to a procedure that enriched and purified the naive $CD4^+CD62L^+$ helper T cells by an indirect immunomagnetic bead purification protocol according to the manufacturer's instructions (Miltenyi Biotec, product no.130-093-227).

### *Assay of cytokine responses of lung DC and naive $CD4^+$ OT-II T cells*

To determine the stimulatory function of highly enriched pulmonary myeloid $CD11c^+$ $Nrf2^{-/-}$ DCs as compared with $Nrf2^{+/+}$ DC counterparts, DCs were exposed to PM (at 10 μg/ml) for 48 h, washed in complete culture medium, and then seeded into 24-well plates in duplicate at a density of $5 \times 10^4$ DCs per well at 500 μl/well. DC were cocultured with $2.5 \times 10^5$ naive $CD4^+CD62L^+$ T cells per well also at 500 μl/well for a total volume of 1.0 ml at a stimulator to responder cell ratio of 1:5, respectively. Cell culture supernatants were harvested after 6 days and quantified by conventional ELISA for the elaboration of either a Th1-type response (IL-12p70, with a sensitivity limit of 7.2 pg/ml obtained from Invitrogen-BioSource, and IFN-γ, with a sensitivity limit of 5.6 pg/ml obtained from BD Biosciences-BD Pharmingen) or a Th2-type immune response (IL-5 and IL-13, both with a sensitivity limit of 4 pg/ml and obtained from eBioscience). Data were collected from duplicate measures in the ELISA platforms described above and defined as mean picograms of secreted cytokine per milliliter.

### *Analysis of extracellular Ag uptake by DCs*

The uptake of FITC-conjugated dextran (DX) (40 kDa; Molecular Probes) by resting or activated DCs was measured by our previously published procedure (2, 31). Resting or activated DCs (as described above) were washed and then incubated in complete culture medium plus 1 mg/ml FITC-DX for 0, 10, 20, 40, and 80 min at 37°C (to measure energy-dependent uptake) or at 4°C to monitor the background fluorescence of the receptor and cell membrane-immobilized FITC-DX that could not be taken up into the cell at this temperature. Active uptake of FITC-DX by cells at 37°C was determined by subtracting the background geometric MFI of DC labeled with FITC-DX at 4°C from the MFI of FITC-DX that was specifically taken up by DC at 37°C (2, 31).

### *Determination of free radical generation in activated DCs*

We quantified free radical production in DC as previously described (32, 33). This assay quantifies the oxidation of nonfluorescent 2′,7′-dichlorofluorescein diacetate (DCFH-DA; Eastman-Kodak) to fluorescent dichlorofluorescein (DCF) in the presence of intracellularly accumulated hydrogen peroxide. On day 8 of culture, immature DCs were assayed for free radical production. This was done by first loading 200 μl of a DC suspension ($2.0 \times 10^5$ cells total) with 100 μl of 5 mM (final concentration) DCFH-DA diluted in PBSg buffer (pH 7.4) (10 mM HEPES, 0.1% (w/v) gelatin, and 10 mM D-glucose) at 37°C for 15 min with agitation. DC were then stimulated with 200 μl of the following agents in control diluent: control diluent alone (PBSg (pH 7.4)), APM (10 μg/ml), carbon black particles (10 μg/ml, as negative control), or the positive controls LPS (100 ng/ml) or CD40 ligand (CD40L) trimer (50 ng/ml). Samples were stimulated for 80 min and then washed, suspended in 1.0% (v/v) paraformaldehyde in FACS buffer, and read on a FACSCalibur flow cytometer using CellQuest 3.1 software (BD Biosciences). We acquired MFI data in the FL1 channel of intracellular DCF fluorescence in real time and transformed it into the percentage increase in respiratory burst activity relative to non-DCFH-DA-loaded resting/nonstimulated DCs for each time point.

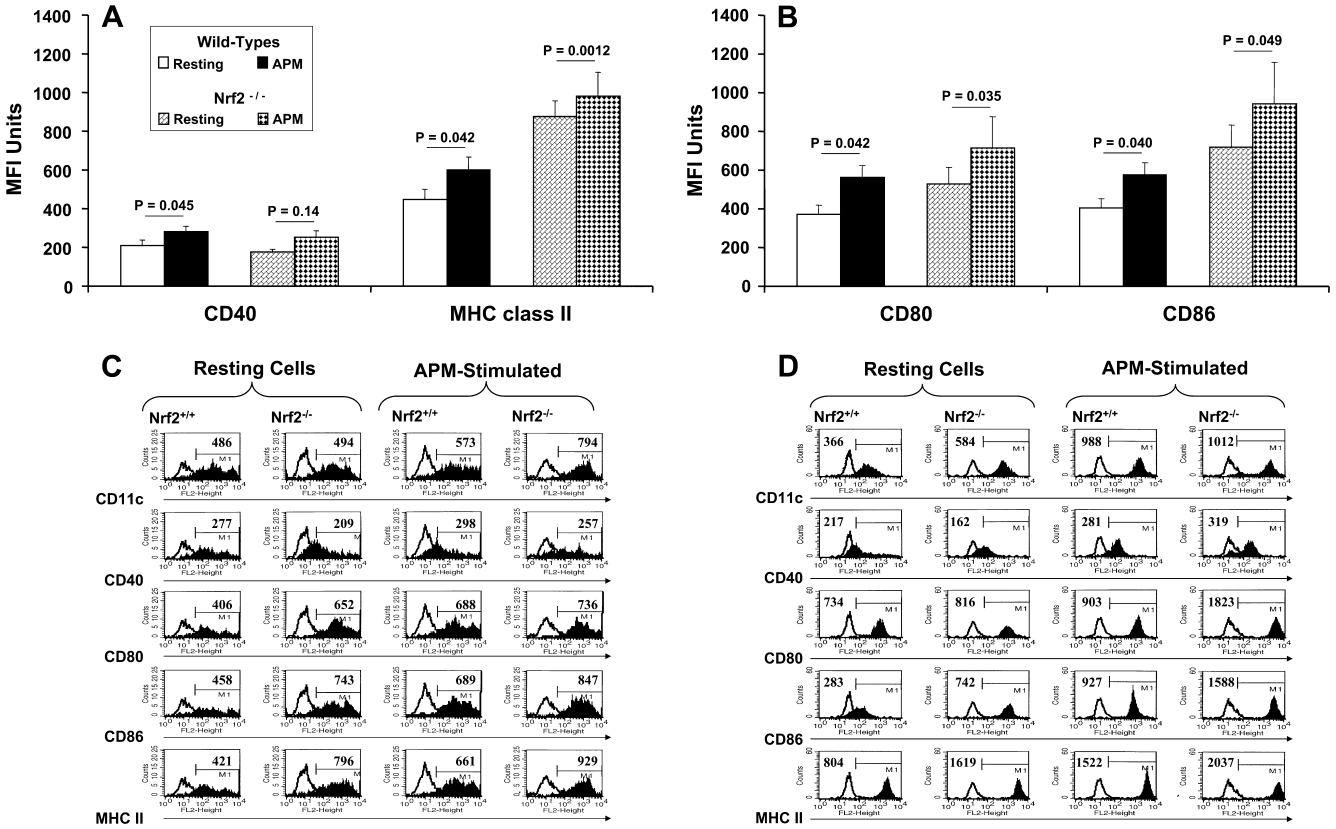


**FIGURE 2.** Flow cytometric determination of cell surface expression of function-associated molecules by bone marrow-derived DCs and purified lung DCs. *A* and *B*, Bone marrow-derived DCs from *Nrf2*$^{+/+}$ and *Nrf2*$^{-/-}$ mice were stimulated in vitro with particulate matter at 10 $\mu$g/ml for 48 h and surface expressions of CD40 and MHC class II (*A*) CD80 and CD86 (*B*) were determined by multiparameter flow cytometry. *C*, In addition, flow histograms of those cell surface markers present on bone marrow-derived DCs of *Nrf2*$^{+/+}$ and *Nrf2*$^{-/-}$ mice from one of the experiments is shown. *D*, Expressions of CD11c, CD40, CD80, CD86, and MHC class II were found on highly purified lung DCs of *Nrf2*$^{+/+}$ and *Nrf2*$^{-/-}$ mice. Data are described as geometric mean ± SD of data collected as MFI from $n = 6$ age- and sex-matched mice per group. Data inserted in the representative flow histograms is also defined as geometric MFI units. Absolute levels of significance ($p$ values) are shown in the figures.

### *Determination of oxidative stress in activated DCs*

We measured mitochondria-derived $H_2O_2$ by chemiluminescence from the luminol (5-amino-2,3-dihydro-1,4-phthalazinedione) reagent using a Berthold Biolumat LB9505 luminometer (PerkinElmer) as described (34). To detect extracellular $H_2O_2$, 10 $\mu$M luminol and 10 $\mu$g/ml HRP were added to 1 ml of PBS (supplemented with 2.5 mM $MgCl_2$ and 5 mg of glucose) containing $1 \times 10^6$ immature DCs and 10 $\mu$g/ml APM. Resting, nonstimulated DCs were used as control. Immediately following the addition of luminol and HRP, we measured the resultant chemiluminescence continuously at 37°C for 60 min. We expressed the data from these experiments as an integrated area under the curve and as mean ± SD from the product of three independent experiments.

### *Determination of Nrf2-regulated antioxidant genes in DCs*

We used quantitative real-time PCR to measure the mRNA levels of *Nrf2*-regulated genes using a previous published procedure (25). We measured the expression levels of the glutathione cysteine ligase catalytic subunit (GCLc), the GCLc modifier subunit (GCLm), and heme oxygenase-1 (HO-1) in DCs using commercially available assay kits (Applied Biosystems). Quantitative RT-PCR was performed using the fluorescent dye SYBR Green master mix following standard protocols on an ABI PRISM 7900 system (Applied Biosystems). Total RNA was extracted from DCs and used for first-strand cDNA synthesis. The reverse transcription reaction was performed with 1 $\mu$g of DNase-treated total RNA, 0.5 $\mu$g of anchored oligo$(dT)_{15}$ primer, and 500 $\mu$M dNTPs (Invitrogen). The levels of cDNA for GAPDH or each antioxidant gene generated from total cellular RNA were calculated by using standard curves generated with cDNAs for GAPDH or each antioxidant gene in which there was a linear relationship between the number of cycles required to exceed the threshold and the number of copies of cDNA added. The data were analyzed using the sequence detector software SDS 2.0 (Applied Biosystems). All PCRs were performed in triplicate.

### *Data analysis*

We expressed data as mean ± SD, and these were the product of two (endocytosis assays) to six independent experiments as indicated (at least three mice per genotype were used for each independent experiment). Comparisons between paired and unpaired data were tested for significant differences using one- and two-way ANOVA, Student's $t$ test, and post hoc correction according to the Bonferroni method. Statistical significance was set at an alpha value of at least $p < 0.05$ as indicated. Statistical measurements were done using SigmaStat version 2.03 software and Microsoft Excel statistical analysis software.

## Results

### *Bone marrow and pulmonary DC expression of function-associated molecules*

To test the hypothesis that PM differentially activates *Nrf2*$^{+/+}$ as compared with *Nrf2*$^{-/-}$ DC, we exposed DC to PM and analyzed the expression of CD11c, CD40, CD80, CD86, and MHC class II by flow cytometry (Fig. 2). In the first series of experiments, we enumerated cell surface expression of these markers in DCs derived from bone marrow progenitors (Fig. 2, *A–C*). In addition, in the second series of experiments we measured the cell surface expression of activation markers on freshly isolated and highly purified PDCA-1 $^{-}$CD11c$^{+}$ myeloid lung DCs (Fig. 2*D*).

Although the resting expression of CD40 was similar between genotypes (Fig. 2, *A* and *C*), the resting expression of MHC class II was somewhat greater on *Nrf2*$^{-/-}$ DCs ($p = 0.079$; Fig. 2, *A* and *C*). Stimulation of DCs augmented the expression of both CD40 and MHC class II (Fig. 2*A*) on *Nrf2*$^{+/+}$ as well as *Nrf2*$^{-/-}$

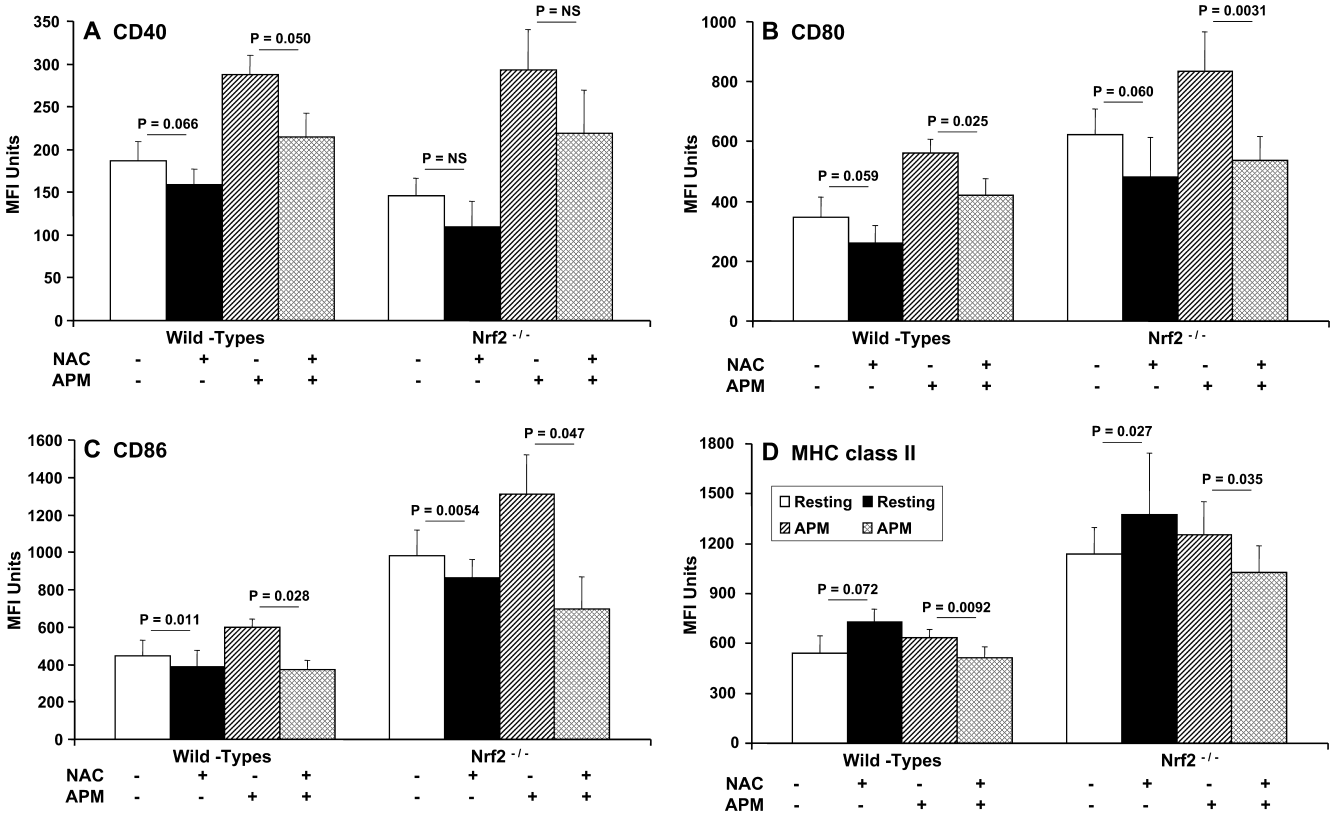


**FIGURE 3.** Flow cytometric quantitation of function-associated molecule expression by DCs showing the effects of NAC on PM-induced alterations in cell surface expression of CD40 (*A*), CD80 (*B*), CD86 (*C*), and MHC class II (*D*) on bone marrow-derived DCs from $Nrf2^{+/+}$ and $Nrf2^{-/-}$ mice. Data shown are mean ± SD of geometric MFI from $n = 6$ age- and sex-matched mice per group. Levels of tests of significance between treatments are shown and are as described in the text.

DCs with the highest levels of MHC class II still evident on $Nrf2^{-/-}$ DCs (Fig. 2*A*). The resting expression of CD80 ($p = 0.086$) and CD86 ($p = 0.068$; Fig. 2, *B* and *C*) was lower on $Nrf2^{+/+}$ as compared with $Nrf2^{-/-}$ DC. This was concordant with our observations made for MHC class II. Stimulation of DC with PM augmented the expression of both CD80 and CD86 by $Nrf2^{+/+}$ as compared with $Nrf2^{-/-}$ DC (Fig. 2, *B* and *C*), and although there were no statistically significant differences between genotypes in the expression of CD80, after the exposure of DCs to PM the expression of CD86 was markedly greater on $Nrf2^{-/-}$ DCs as compared with their wt counterparts (Fig. 2, *B* and *C*; $p = 0.0023$).

We repeated the above studies in lung DCs. We found that there were marked differences in the constitutive (resting) expression of cell surface function-associated molecules between genotypes (Fig. 2*D*). Although the expression of CD40 was not statistically different between $Nrf2^{-/-}$ lung DCs and their wt counterparts, the expression of CD11c and CD80 (to a lesser extent) and the expression of CD86 and MHC class II in particular were markedly greater on lung DCs from $Nrf2^{-/-}$ DCs as compared with their wt counterparts (Fig. 2*D*). Thus, $Nrf2^{-/-}$ lung DCs were at a constitutively greater level of activation in the resting state than $Nrf2^{+/+}$ lung DCs.

Upn the activation of lung DCs by APM we observed a striking disparity in the overall hyperresponsiveness of $Nrf2^{-/-}$ DC as compared with the expected modest augmentation in cell surface markers by $Nrf2^{+/+}$ DCs (Fig. 2*D*). In both $Nrf2^{+/+}$ and $Nrf2^{-/-}$ lung DCs, the expression of CD11c was augmented upon activation by APM. There was only modest augmentation in CD40 expression upon the stimulation of $Nrf2^{+/+}$ DCs with APM, whereas the expression of this receptor doubled upon the activation of $Nrf2^{-/-}$ DCs by APM (Fig. 2*D*). In addition, although there was a modest up-regulation in the expression of CD80 and a more significant augmentation in both CD86 and MHC class II expression upon the stimulation of $Nrf2^{+/+}$ DC with APM, we observed remarkable responses by $Nrf2^{-/-}$ DCs upon activation by APM (Fig. 2*D*). Expression levels of CD80, CD86, and MHC class II were all markedly enhanced as compared with those for resting DCs as well as when contrasted with their wt counterparts. These observations were concordant, at least in part, with those observations made for the functional response of bone marrow-derived DCs to particulate matter exposure (Fig. 2, *A–C*).

### *Effects of NAC on receptor expression by DCs*

NAC is a widely used antioxidant molecule that possesses immunomodulatory effects, including an ability to dampen the expression of cell surface-expressed molecules upon the activation of DC. We were interested in determining the ability of NAC to suppress PM-mediated DC activation. Thus, in a separate series of experiments (Fig. 3) we pretreated DCs with 5 mM NAC for 1 h and then exposed DCs to PM for 48 h before phenotypic analysis. First, we confirmed that $Nrf2^{+/+}$ as well as $Nrf2^{-/-}$ DCs responded appropriately to stimulation with PM, as we had shown previously in our initial observations discussed above (Fig. 2) for all surface markers studied (Fig. 3). Next, we stimulated DCs with or without PM in the presence or absence of NAC as shown (Fig. 3).

In resting $Nrf2^{+/+}$ wt DC, NAC inhibited the expression of CD40 (Fig. 3*A*), CD80 (Fig. 3*B*), and CD86 (Fig. 3*C*) while at the same time promoting the expression of MHC class II (Fig. 3*D*).

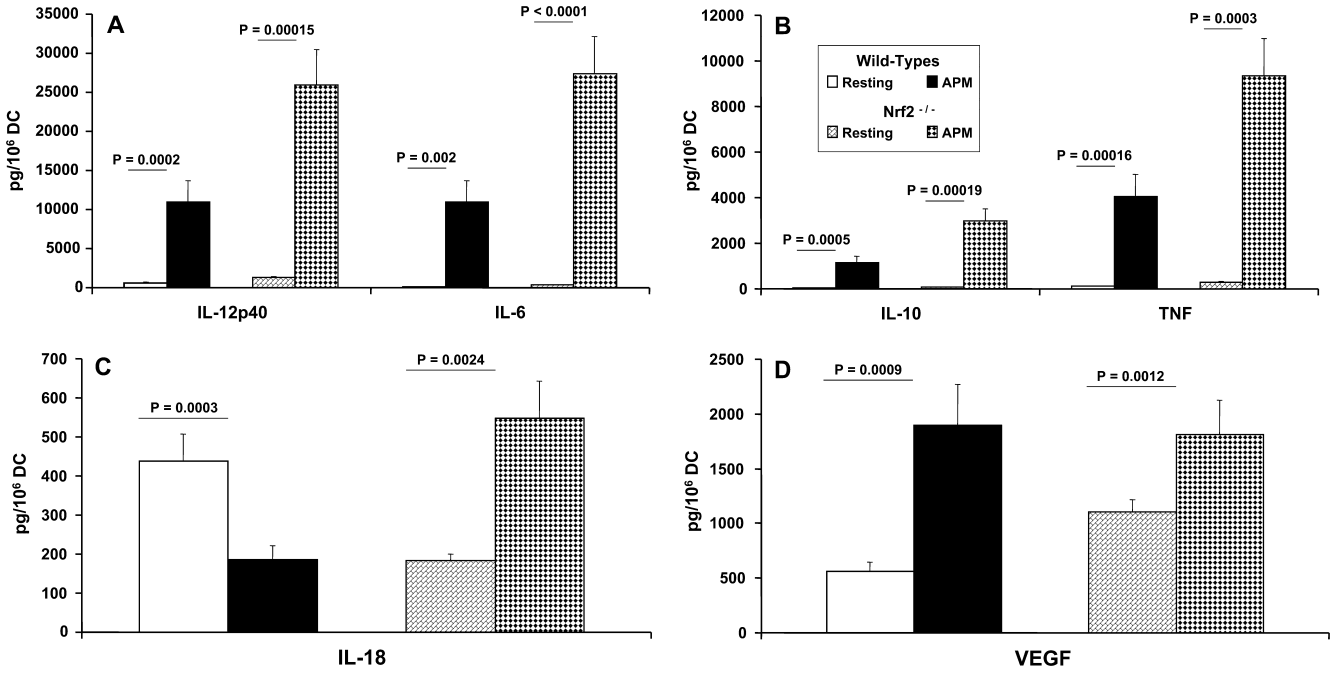


**FIGURE 4.** Quantitation of inflammatory cytokine production by PM-exposed DCs from *Nrf2*$^{+/+}$ and *Nrf2*$^{-/-}$ mice. The secretion of immunoreactive IL-12p70 and IL-6 (*A*), IL-10 and TNF (*B*), as well as IL-18 (*C*) and VEGF (*D*) is shown. Bone marrow-derived DCs from the indicated strains were incubated with or without (Resting) particulate matter for 48 h, followed by analysis of cell-free supernatants by commercially available ELISA. Data are expressed as picograms per million cells and are the product of the mean ± SD of $n = 6$ sex- and age-matched mice per group.

Although most of these effects of NAC were evident in *Nrf2*$^{-/-}$ DCs, we did not see a statistically significant decrease in CD40 expression in NAC treated *Nrf2*$^{-/-}$ DCs and a modest diminution in expression of CD40 by their wt counterparts ($p = 0.066$; Fig. 3*A*). However, a consistent observation was that in PM-stimulated *Nrf2*$^{+/+}$ and *Nrf2*$^{-/-}$ DCs NAC attenuated the PM-driven enhancement of MHC class II, CD80, and CD86 expression. However, only in *Nrf2*$^{+/+}$ DCs did NAC significantly attenuate CD40 expression ($p = 0.05$; Fig. 3*A*). Thus, CD40 expression in resting and PM-stimulated *Nrf2*$^{-/-}$ DCs appeared to be refractory to NAC (Fig. 3*A*).

### *Particulate matter directs an Nrf-2-dependent pattern of cytokine production by DCs*

We examined a panel of cytokines known to be important in allergic diseases and the differentiation of T cells. Thus, we assessed the constitutive ability of *Nrf2*$^{+/+}$ and *Nrf2*$^{-/-}$ knockout DCs to release inflammatory cytokines in the resting state and following activation by PM (Fig. 4). We found that *Nrf2*$^{+/+}$ DCs released minimal levels of IL-12p40 and IL-6 (Fig. 4*A*) and IL-10 and TNF-$\alpha$ (Fig. 4*B*), yet proportionately elevated levels of IL-18 (Fig. 4*C*) and VEGF (Fig. 4*D*) in the resting state. By contrast, resting *Nrf2*$^{-/-}$ DCs constitutively released greater levels of IL-12p40 ($p = 0.0012$), IL-6 ($p = 0.0006$), IL-10 ($p = 0.0038$), and TNF-$\alpha$ ($p = 0.0001$), as well as VEGF ($p = 0.001$), than their wt counterparts, although the levels constitutively released by both *Nrf2*$^{+/+}$ and *Nrf2*$^{-/-}$ DCs were modest (Fig. 4). By contrast, *Nrf2*$^{-/-}$ DCs released constitutively lower levels of IL-18 than their *Nrf2*$^{+/+}$ DC counterparts (Fig. 4*C*; $p = 0.0024$) by mechanisms that may be dependent in part on *Nrf2* activity.

Activation of both *Nrf2*$^{+/+}$ and *Nrf2*$^{-/-}$ DC with PM enhanced the secretion of all cytokines measured with the exception of IL-18 (Fig. 4, *A–C*). In response to PM stimulation, *Nrf2*$^{+/+}$ DCs secreted markedly less IL-18 as compared with resting DCs (Fig. 4*C*; $p = 0.0003$). This contrasted with the up-regulation in IL-18 production by *Nrf2*$^{-/-}$ DCs as compared with resting DCs (Fig. 4*C*; $p = 0.00038$), further supporting the notion that the production of IL-18 by DCs is dependent on the expression of *Nrf2*. Under conditions of disrupted *Nrf2* we saw suppressed constitutive expression of IL-18 and enhanced production of this cytokine following stimulation with PM, whereas in wt DCs the converse was true. This is a novel and previously unreported effect.

Moreover, we repeated the above studies in freshly isolated, highly purified CD11c$^{+}$ myeloid lung DCs by investigating the time-dependent production of the secretion of TNF-$\alpha$ and IL-12p40, representing two cytokines thought to be important in pulmonary inflammation and the inflammatory chemokine KC/CXCL1 (Fig. 5, *A* and *B*, respectively). The secretion of TNF-$\alpha$ and IL-12p40 are important in mouse models of pulmonary and allergic inflammation (35–38). In addition, we studied the temporal secretion of KC (Fig. 5*B*) in response to PM (10 $\mu$g/ml), because this chemokine is an important mediator in lung inflammation and we have also found that secretion of KC is a very sensitive marker of murine myeloid DC activation (39, 40).

In our experiments, we found that peak secretion of TNF and IL-12p40 by *Nrf2*$^{-/-}$ and *Nrf2*$^{+/+}$ DC occurred 48 h after stimulation by PM (Fig. 5). However, as was concordant for *Nrf2*$^{-/-}$ bone marrow-derived DCs, their pulmonary myeloid DC counterparts also exhibited markedly greater levels of TNF and IL-12p40 secretion than was observed for wt pulmonary DC at all of the time points studied. In addition, the constitutive secretion of both cytokines by *Nrf2*$^{-/-}$ DCs in the resting state (time 0 h) was also markedly greater than the levels observed for *Nrf2*$^{+/+}$ DCs (Fig. 5), consistent with the observations made for bone marrow-derived DCs. By contrast, peak secretion of KC followed a more rapid pattern of secretion that peaked at 24 h poststimulation for both genotypes (Fig. 5*B*). Concordant with the absolute levels of TNF and IL-12p40 secretion, we found that *Nrf2*$^{-/-}$ DCs secreted significantly greater levels of KC both constitutively in the resting state and upon activation by PM. Thus, both bone marrow-derived

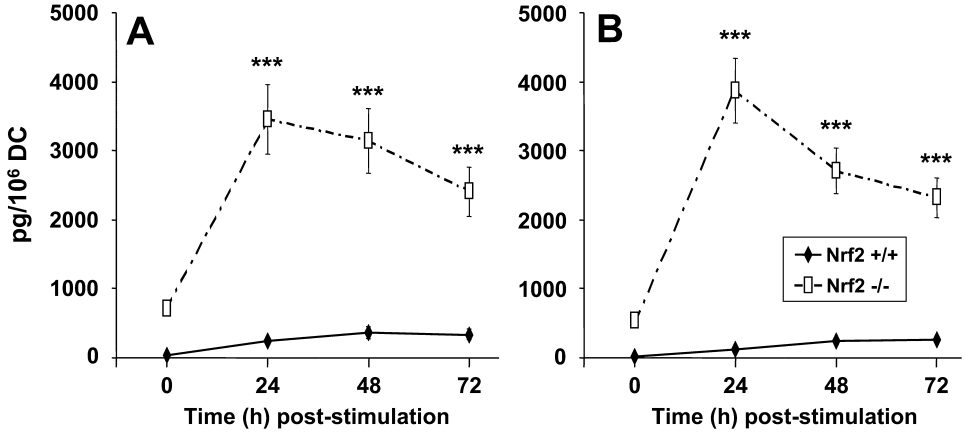


**FIGURE 5.** An analysis of the time-dependent secretion of inflammatory cytokines of resting (unstimulated) lung DCs from $Nrf2^{+/+}$ and $Nrf2^{-/-}$ mice as compared with PM-exposed DCs. The secretion of TNF-$\alpha$ (*A*) and KC (*B*) was assessed by commercial ELISA protocols at 24, 48, and 72 h following the exposure of DCs to PM. Data are described as mean picograms per million DCs ± 1 SD. Levels of significance as indicated (***) are $p < 0.01$.

and pulmonary myeloid DCs from $Nrf2^{-/-}$ mice possess a heightened state of inflammatory activation.

### *Effects of NAC on inflammatory cytokine production by DCs*

In a separate series of experiments, we next looked at the effects of NAC on cytokine production by both $Nrf2^{+/+}$ and $Nrf2^{-/-}$ DCs in the resting state as well as following PM activation (Table I). First, we confirmed the cytokine responses of both $Nrf2^{+/+}$ and $Nrf2^{-/-}$ DCs as defined in Fig. 4. Second, we pretreated DCs with 5 mM NAC for 1 h and then exposed them to PM for 48 h before assessing the secretion of cytokines by commercial ELISA (Table I). NAC provoked a complex pattern of cytokine production. In *Nrf2* wt DCs, NAC enhanced the secretion of IL-6, IL-10, IL-18, and VEGF and suppressed the secretion of IL-12p40 and TNF. By contrast, in $Nrf2^{-/-}$ DCs NAC enhanced the secretion of TNF-$\alpha$ and VEGF and dampened the production of IL-12p40, IL-6, IL-10, and IL-18 (Table I).

Although cytokine production by both $Nrf2^{+/+}$ and $Nrf2^{-/-}$ DC populations responded appropriately following exposure to PM (Table I), NAC significantly attenuated the production of most of the cytokines by PM-exposed DCs. However, the production of TNF-$\alpha$ by PM-exposed $Nrf2^{-/-}$ DCs remained unaltered after NAC treatment, whereas the production of VEGF remained unaffected by NAC in $Nrf2^{+/+}$ DCs. It is currently unknown why the secretion of TNF-$\alpha$ and VEGF should show such differences between $Nrf2^{+/+}$ and $Nrf2^{-/-}$ DCs following PM exposure in the presence of NAC (Table I). This pattern of cytokines secreted by PM-exposed DCs is unusual and different from that associated with classical activators of DCs such as LPS or CD40L, which typically induce IL-6, TNF-$\alpha$, and IL-12 in a coordinated fashion.

### *Pulmonary myeloid $Nrf2^{-/-}$ DCs promote Th2-like cytokine responses by naive CD4 T cells*

In 6-day differentiated cocultures of highly purified naive $CD4^+CD62L^+$ T cells stimulated by either $Nrf2^{-/-}$ pulmonary myeloid DCs or their wt counterparts, we were interested in determining how PM pre-exposure affected the ability of DCs to influence T cell activation, especially the production of Th1 vs Th2 cytokines (Fig. 6). To discriminate Th2 cytokine responses we measured the secretion of IL-13 and IL-5 (Fig. 6*A*) and, by contrast, to identify Th1 cytokine responses we measured the secretion of IL-12p70 and IFN-$\gamma$ (Fig. 6*B*). To better appreciate the bias of the Th2-type cytokine responsiveness of PM-exposed $Nrf2^{-/-}$ DCs contrasted with that of $Nrf2^{+/+}$ DCs, we compared the levels of IL-13 secretion relative to the levels of either IFN-$\gamma$ or IL-12p70 by ratiometric analysis (Fig. 6*C*).

We observed that the secretion of IL-13 was enhanced in PM-stimulated pulmonary DC/T cell cocultures. However, the amounts seen in coculture with $Nrf2^{-/-}$ DCs were at least 2.8-fold greater than those seen using wt DC in cocultures (Fig. 6*A*). Similarly,

Table I. *Effects of NAC on cytokine production by both $Nrf2^{+/+}$ and $Nrf2^{-/-}$ DCs in the resting state as well as following PM activation*[a]

| Treatment | IL-12p40 | IL-6 | IL-10 | TNF | IL-18 | VEGF |
|---|---|---|---|---|---|---|
| Resting $Nrf2^{+/+}$ | 481.9 ± 128.4 | 122.3 ± 22.4 | 15.1 ± 35.6 | 110.6 ± 9.1 | 430.8 ± 37.3 | 597.4 ± 186.2 |
| Resting $Nrf2^{+/+}$ NAC | 352.4 ± 193.1 ($p$ = 0.017) | 171.3 ± 35.6 ($p$ = 0.048) | 79.5 ± 12.3 ($p$ = 0.021) | 93.5 ± 9.8 ($p$ = 0.021) | 603.9 ± 104.2 ($p$ = 0.047) | 652.5 ± 181.3 ($p$ = NS) |
| Resting $Nrf2^{-/-}$ | 1004 ± 128.9 | 356.6 ± 39.3 | 45.5 ± 25.4 | 288.6 ± 30.6 | 200.5 ± 37.7 | 1143 ± 131.2 |
| Resting $Nrf2^{-/-}$ NAC | 423.1 ± 112.7 ($p$ = 0.004) | 97.7 ± 12.5 ($p$ = 0.0039) | 30.1 ± 21.1 ($p$ = 0.042) | 409.4 ± 85.5 ($p$ = 0.063) | 74.9 ± 18.8 ($p$ = 0.021) | 1417 ± 144.1 ($p$ = 0.01) |
| APM Resting $Nrf2^{+/+}$ | 9895 ± 1966 | 11467 ± 3590 | 971.8 ± 236.1 | 4178 ± 452.6 | 206.9 ± 96.6 | 1615 ± 286.6 |
| APM Resting $Nrf2^{+/+}$ NAC | 947.4 ± 161.7 ($p$ = 0.001) | 5638 ± 1791 ($p$ = 0.065) | 52.9 ± 7.2 ($p$ = 0.0026) | 1547 ± 436.6 ($p$ = 0.002) | 23.2 ± 9.5 ($p$ = 0.031) | 1460 ± 122.1 ($p$ = NS) |
| APM Resting $Nrf2^{-/-}$ | 29572 ± 3764 | 28170 ± 2355 | 2535 ± 732.9 | 9825 ± 1873 | 603.3 ± 98.2 | 2066 ± 473.6 |
| APM Resting $Nrf2^{-/-}$ NAC | 24835 ± 2966 ($p$ = 0.017) | 18570 ± 2030 ($p$ = 0.024) | 1889 ± 455.1 ($p$ = 0.059) | 9272 ± 1174 ($p$ = ns) | 161.2 ± 50.7 ($p$ = 0.004) | 1294 ± 250.2 ($p$ = 0.034) |

[a] Immature DCs were stimulated in the absence or presence of APM (10 $\mu$g/ml) with or without NAC (5 mM) for 48 h. After this stimulation, we analyzed DC cytokine secretion by ELISA. To maximize antioxidant activity, cells were pretreated with NAC for 1 h prior to addition of APM for the remaining 48-h incubation period. Levels of cytokine secretion are shown as mean picograms per million cells ± SD ($n$ = 3 independent experiments). The $p$ values for levels of significance between pairs of data are shown in parenthesis for each cytokine. This was done for resting unstimulated DCs in the absence or presence of NAC for both $Nrf2^{+/+}$ and $Nrf2^{-/-}$ DCs and again for DCs stimulated without or with APM in the absence or presence of NAC.

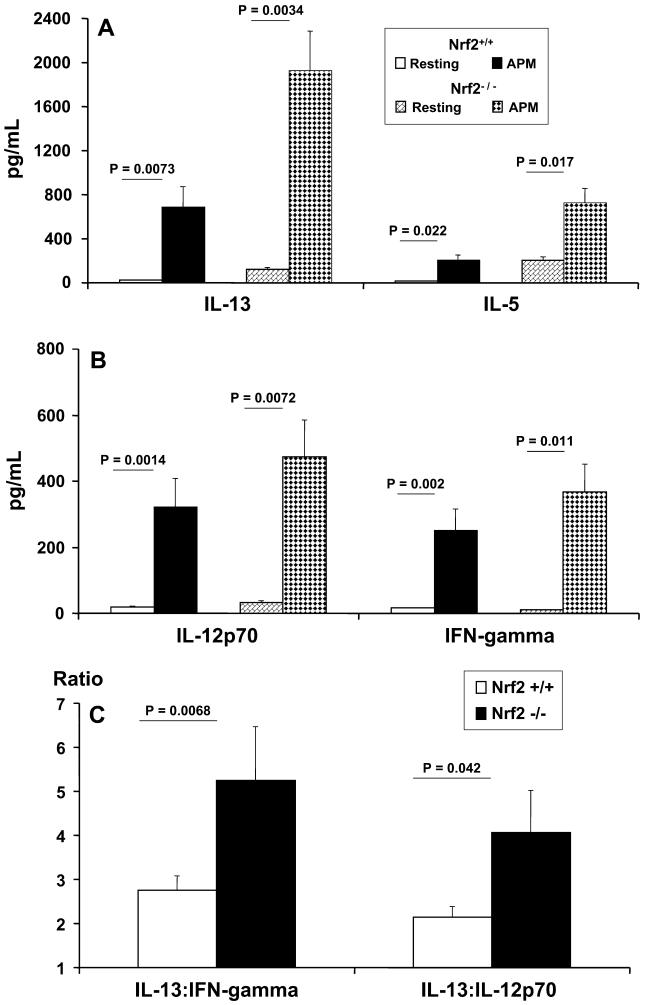


**FIGURE 6.** Determination of Th1-type (IL-12p70 and IFN-γ) vs Th2-type (IL-13 and IL-5) cytokines by OVA-pulsed (50 μg/ml) lung DCs from *Nrf2*$^{+/+}$ and *Nrf2*$^{-/-}$ mice and coculture with naive CD4$^{+}$CD45RA$^{+}$ allogeneic OT-II T cells at a stimulator (DC) to responder T cell ratio of 1:5 (see *Materials and Methods*). The secretion of IL-13 and IL-5 (*A*) and the secretion IL-12p70 and IFN-γ (*B*) are shown. In addition, a ratiometric analysis of the secretion of IL-13 produced by PM-stimulated Nrf2$^{+/+}$ and Nrf2$^{-/-}$ DCs relative to either IFN-γ or IL-12p70 secretion is shown (*C*). Data are described as picograms of cytokine per milliliter produced in the coculture.

although PM-stimulated pulmonary DC promoted enhanced production of IL-5 in coculture with OT-II T cells, the relative amounts seen in *Nrf2*$^{-/-}$ DC cocultures were at least 3.5-fold greater than those seen in wt DC cocultures (Fig. 6*A*). These data suggest an enhanced and default pro-Th2 bias of *Nrf2*$^{-/-}$ DCs seen upon contact with naive CD4$^{+}$ T cells. Although PM-stimulated *Nrf2*$^{+/+}$ DC also enhanced the production of IL-13 and IL-5 by naive CD4$^{+}$ T cells, the levels secreted were markedly lower. In addition, resting *Nrf2*$^{-/-}$ DCs stimulated greater levels of both IL-13 and IL-5 than their wt counterparts on coculture with naive CD4$^{+}$ T cells, supporting our suggestion of a pro-Th2 bias in *Nrf2*$^{-/-}$ DCs (Fig. 6*A*).

PM-exposed DCs also stimulated enhanced production of both Th1-type cytokines, IL-12p70 and IFN-γ (Fig. 6*B*). However, in contrast to the markedly greater levels of Th2-type cytokines that we found in *Nrf2*$^{-/-}$ DC/T cell cocultures as compared with their wt counterparts, this was not true for the observed levels of IL-12p70 and IFN-γ between genotypes (Fig. 6*B*). In this case, we found that there was only a 1.5-fold greater level of IL-12p70 secretion and IFN-γ in cocultures stimulated by *Nrf2*$^{-/-}$ DCs as compared with cocultures stimulated by *Nrf2*$^{+/+}$ DCs (Fig. 6*B*).

When expressing the data described as a ratio of IL-13 secretion relative to either IL-12p70 or IFN-γ (Fig. 6*C*), we found that those cocultures stimulated by PM-exposed Nrf2$^{-/-}$ DCs indeed promoted a more dramatic pro-Th2 bias of cytokine responsiveness by naive CD4$^{+}$ T cells than did their wt counterparts.

### *APM and differential Ag uptake by DCs*

During the functional maturation of DCs, there is an initial augmentation of Ag uptake followed by a diminished internalization of uptake in favor of Ag processing and presentation. To determine the endocytic activity of DCs, we measured the time-dependent uptake of dextran as a model exogenous Ag (see *Materials and Methods*).

In the resting state (Fig. 7*A*) we found that both *Nrf2*$^{+/+}$ and *Nrf2*$^{-/-}$ efficiently took up Ag, although DCs from *Nrf2*$^{+/+}$ mice showed a lowered ability to take up FITC-DX as compared with their *Nrf2*$^{-/-}$ counterparts that was significantly different at 30 min. We also measured the ability of DCs to take up dextran following activation with PM (Fig. 7*B*). Under these circumstances, *Nrf2*$^{+/+}$ DCs retained an efficient time-dependent ability to take up exogenous Ag as well as an improved ability to do so at the conclusion of the assay as compared with their resting counterparts ($p = 0.084$; Fig. 7). By contrast, PM-exposed *Nrf2*$^{-/-}$ DCs exhibited a greatly diminished ability to take up exogenous FITC-DX as compared with PM-exposed *Nrf2*$^{+/+}$ DCs (Fig. 7*B*) as well as their resting counterparts (Fig. 7*A*; $p \leq 0.013$). This highlights a functional difference between murine DCs that express and those that lack *Nrf2* gene expression and suggests that the disruption of

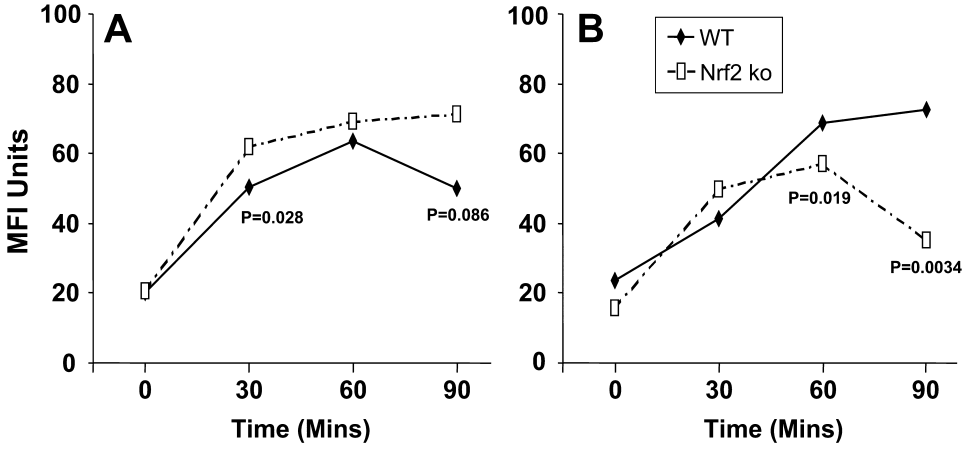


**FIGURE 7.** Flow cytometric quantitation of the endocytic uptake of FITC-DX (40 kDa) by resting (*A*) or PM-exposed (*B*) DCs from *Nrf2*$^{+/+}$ (WT, wild type) and *Nrf2*$^{-/-}$ (Nrf2 ko (knockout)) mice. The time-dependent endocytosis of FITC-dextran is shown and levels of tests of significance between *Nrf2*$^{+/+}$ as compared with the *Nrf2*$^{-/-}$ DCs are also described for comparison. Data are described as geometric MFI.

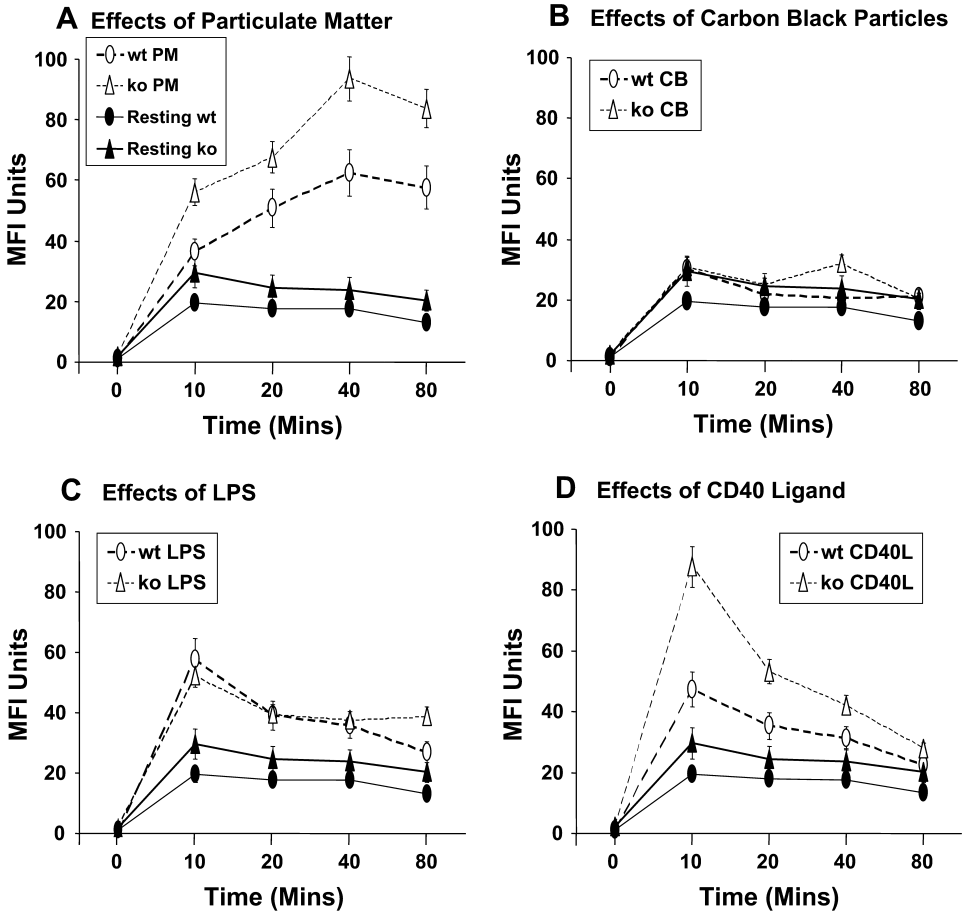


**FIGURE 8.** Flow cytometric quantitation of $H_2O_2$ production and accumulation of resting DCs as compared with PM-exposed DCs. Data are geometric MFI ± SD as a function of DCF fluorescence (oxidized DCFH-DA). The respiratory burst of DCs derived from *Nrf2*$^{+/+}$ and *Nrf2*$^{-/-}$ mice is shown following stimulation with PM (*A*) and as compared with the negative control carbon black (CB) particulates (*B*), bacterial LPS/endotoxin (*C*), and trimeric CD40L (*D*). ko, Knockout.

*Nrf2*-mediated signaling mechanisms may impair endocytosis by activated DCs (See *Discussion*).

### *PM-induced oxidative stress in Nrf2-deficient DCs*

We assessed oxidative stress activity in resting and APM-exposed DCs by quantifying intracellular $H_2O_2$ accumulation. We did this by using the reporter molecule DCFH-DA, which is nonfluorescent in the unexcited state but becomes rapidly oxidized during normal basal metabolism and even more so during cellular activation. DCFH-DA is highly specific for $H_2O_2$ accumulation and is oxidized by products of NO reacting with oxygen-free radicals. Thus, for this reason DCFH-DA is an important reporter of alterations of the intracellular redox state of cells.

Both resting *Nrf2*$^{+/+}$ and *Nrf2*$^{-/-}$ DCs exhibited a basal level of $H_2O_2$ production that was somewhat elevated in *Nrf2*$^{-/-}$ DCs (Fig. 8; $p \leq 0.024$). Activation of DCs with PM (Fig. 8*A*) provoked rapid increases in $H_2O_2$ production in both *Nrf2*$^{+/+}$ and *Nrf2*$^{-/-}$ DCs as compared with resting DCs ($p < 0.001$). The greatest levels of activity were seen in *Nrf2*$^{-/-}$ DCs as compared with their wt counterparts at all time points (Fig. 8*A*; $p < 0.01$). Importantly, we did not observe significant increases in $H_2O_2$ accumulation in DCs exposed to carbon black particles (Fig. 8*B*), indicating that $H_2O_2$ production by DCs was a specific effect of components contained in PM. Also, LPS promoted enhanced $H_2O_2$ accumulation equally well in both *Nrf2*$^{+/+}$ and *Nrf2*$^{-/-}$ DCs as compared with resting DCs (Fig. 8*C*). This was in stark contrast with the responses of *Nrf2*$^{+/+}$ and *Nrf2*$^{-/-}$ DCs to CD40L stimulation (Fig. 8*D*). Under these conditions, we found that *Nrf2*$^{-/-}$ DCs were particularly sensitive to the effects of CD40L as compared with *Nrf2*$^{+/+}$ DCs showing a rapid (within 10 min) and marked increase in $H_2O_2$ production as compared with resting and wt DCs at 10 and 20 min poststimulation ($p < 0.001$, Fig. 8*D*).

We confirmed the effects of PM on DCs independently by measuring a luminol-based oxidative stress assay (Fig. 9). In the current study, we have used this assay to measure $H_2O_2$ formation by DCs in the presence/absence of PM. Concordant with our observations above, we found that while resting DCs did not produce significant amounts of $H_2O_2$ by this assay, PM directed a marked

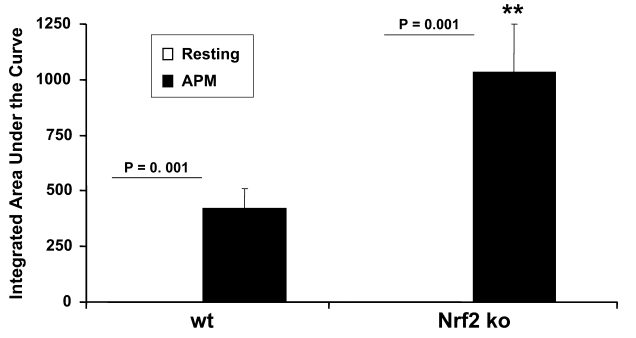


**FIGURE 9.** The effect of PM and the induction of enhanced oxidative stress in *Nrf2*$^{-/-}$ DCs as compared with *Nrf2*$^{+/+}$ DCs. In this assay, real-time $H_2O_2$ formation was measured by a peroxidase luminol chemiluminescence (CL) method. The CL response was initiated by adding 5 $\mu$M luminol and 10 $\mu$g/ml HRP and continuously monitored at 37°C for 1 h. Data are mean ± SD of three independent experiments. Levels of significance between resting and PM-treated DCs are described as absolute values on the figure; ** represents enhanced production of $H_2O_2$ by *Nrf2*$^{-/-}$ DCs as compared with their wt counterparts at $p < 0.001$. ko, Knockout.

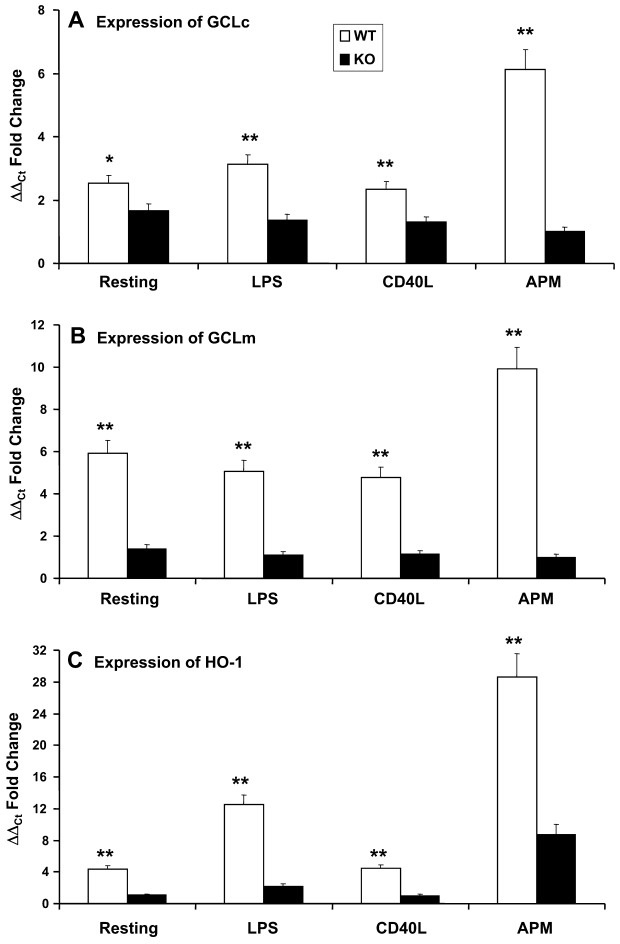


**FIGURE 10.** Increased transcriptional induction of antioxidant genes in $Nrf2^{+/+}$ DCs as compared with $Nrf2^{-/-}$ DC. Quantitative real-time RT-PCR analysis showed increased levels of mRNA for genes such as γGCLc (*A*), γ GCLm (*B*), and HO-1 (*C*) in PM-exposed wt $Nrf2^{+/+}$ DCs as compared with $Nrf2^{-/-}$ DCs. Results are mean ± SD of three independent experiments. Levels of statistical significance (**, $p \leq 0.05$) are for $Nrf2^{+/+}$ DCs as compared with $Nrf2^{-/-}$ DCs. For comparative purposes, the inductions of γGCLc (*A*), γ GCLm (*B*), and HO-1 (*C*) in response to both LPS and trimeric CD40L are shown. In each case, PM was more effective at inducing antioxidant gene expression than either LPS or CD40L in this model. Ct, Cycle threshold.

augmentation in $H_2O_2$ production as compared with resting DCs ($p < 0.001$, Fig. 9). Moreover, luminol-derived chemiluminescence was significantly higher in PM-stimulated $Nrf2^{-/-}$ DCs than the $Nrf2^{+/+}$ counterparts. Thus, using two independent assays we found that PM induced excess oxidative stress in Nrf2-disrupted DCs as compared with $Nrf2^{+/+}$ DCs.

*Attenuation of antioxidant gene expression in Nrf2-defienct DCs*

Oxidative stress may be important in the maturation of DCs. Antioxidants inhibit some aspects of DC maturation. However, very little is known about the expression of antioxidant genes by DCs as a function of their activation and/or maturation state. We therefore assessed the induction of three classic *Nrf2*-regulated genes in $Nrf2^{+/+}$ and $Nrf2^{-/-}$ DCs before or after exposure to PM, namely GCLc (Fig. 10*A*), the GCLc modifier subunit GCLm (Fig. 10*B*), as well as HO-1 (Fig. 10*C*). We found that while LPS and CD40L enhanced the induction of expression of GCLc (3.1- and 2.3-fold, respectively; Fig. 10*A*), PM dramatically augmented the expression of this gene as compared with unstimulated $Nrf2^{+/+}$ DCs (6.1-fold induction; Fig. 10*A*). In $Nrf2^{-/-}$ DCs we observed a lower level of induction of GCLc in response to stimulation by LPS (1.4-fold) or CD40L (1.3-fold), whereas the stimulation of $Nrf2^{-/-}$ DCs with PM was completely without effect (Fig. 10*A*). Under all conditions, the induction of GCLc by $Nrf2^{+/+}$ DCs following exposure to LPS, CD40L, or PM was significantly greater than the levels of induction seen in $Nrf2^{-/-}$ DCs ($p < 0.001$; Fig. 10*A*).

We observed similar responses of DCs at the level of GCLm induction (Fig. 10*B*). In $Nrf2^{+/+}$ DCs, LPS (5.1-fold), CD40L (4.8-fold), and PM (9.92-fold) augmented the induction of this gene to levels that were markedly greater than those in $Nrf2^{-/-}$ DCs ($p < 0.001$, Fig. 10*B*). In addition, the stimulation of $Nrf2^{-/-}$ DCs with PM was completely without effect, and stimulation with LPS or CD40L directed only partial induction (1.11- and 1.14-fold, respectively). Finally, whereas CD40L only modestly induced expression of HO-1 (4.4-fold; Fig. 10*C*) in $Nrf2^{+/+}$ DCs, it failed to induce any expression by $Nrf2^{-/-}$ DCs. By contrast, LPS markedly induced the expression of HO-1 by wt DCs (12.5-fold) and only marginally did so in $Nrf2^{-/-}$ DCs (2.2-fold induction). In $Nrf2^{+/+}$ and $Nrf2^{-/-}$DCs, PM directed a massive induction of HO-1, particularly in $Nrf2^{+/+}$ DCs (28.6- and 8.7-fold respectively).

In summary, $Nrf2^{+/+}$ DCs expressed greater constitutive levels of expression of GCLc, GCLm, and HO-1 as compared with their $Nrf2^{-/-}$ counterparts (Fig. 10). In addition, these data show that PM is a highly potent inducer of three important antioxidant genes in an Nrf2-dependent manner.

## Discussion

The link between innate immunity and subsequent functional responses to environmental particulate exposures, such as ambient urban PM, remains poorly defined. Similarly, the link between PM exposure, antioxidant defense mechanisms, and allergic immunity warrants further investigation. DCs are the key component of the innate immune system that evolved to rapidly sense and respond to diverse environmental stimuli. In this work, we used a well-characterized source of ambient urban PM (1, 2) to probe the role of oxidative stress in DC activation. Oxidative stress plays an important role in promoting DC activation and its functional maturation (19, 41–43).

In the current study, we have provided a comprehensive analysis of the effects of endotoxin-free APM (1, 2) on the functional responses of murine bone marrow-derived DCs as well as pure populations of pulmonary $CD11c^+$ myeloid DCs generated from $Nrf2^{+/+}$ and $Nrf2^{-/-}$ mice. We show that *Nrf2* regulates a physiologically relevant and intrinsic antioxidant defense system that protects DCs from ambient urban particles. Our studies indicate that *Nrf2* plays a previously underappreciated role in innate immunity and suggests that a deficiency of *Nrf2*-dependent pathways may be involved in susceptibility to the adverse health effects of air pollution.

We showed that PM drives many aspects of DC activation that are crucial in innate immunity and host defense. Specifically, when contrasted with $Nrf2^{+/+}$ DCs, we showed that cell surface expression of costimulatory molecules and MHC class II was higher on $Nrf2^{-/-}$ DCs. This indicated that DCs from $Nrf2^{-/-}$ mice were already in a state of relative heightened activation as compared with their wt counterparts, possibly due to oxidant signals generated during their in vitro differentiation. In addition, the cell surface expression of CD80, CD86, and MHC class II could be augmented by PM-exposed $Nrf2^{+/+}$ DCs to levels that were seen on $Nrf2^{-/-}$ DCs. The developmental pathway of DC maturation in $Nrf2^{-/-}$ DCs warrants further investigation, but it does exemplify

the hypothesis that ROS play a crucial role in the maturation of DCs. In addition, our data support the hypothesis that *Nrf2* may guard against inappropriate maturation of DCs until the resting DCs sense and respond to danger signals.

We confirmed the importance of reactive oxidants contributing to the maturation of DCs by using the antioxidant molecule NAC. Treatment of DCs with the antioxidant NAC inhibited the maturation of DCs (43), and this was concordant with our observations. In resting $Nrf2^{+/+}$ DCs we showed that NAC dampened the expression of costimulatory molecules. We also observed enhanced cell surface expression of MHC class II molecules by $Nrf2^{+/+}$ DCs following exposure to NAC. However, in $Nrf2^{-/-}$ DCs the expression of CD40 was unaffected by NAC. This suggests that NAC targets the expression of CD40 in an *Nrf2*-dependent manner. Under these circumstances, it is likely that the DC is held in a state of immaturity and is poised to sample and associate endogenously processed Ag by MHC class II. Others have shown that ROS serve a critical role in the activation of DCs as well as the inhibition of DC maturation by antioxidants (16, 43–45). In human monocyte-derived DCs, ROS generated by xanthine oxidase induced early phenotypic maturation of augmented cell surface expression of the costimulatory molecules CD80 and CD86 as well as the DC maturation marker CD83. NAC also attenuated the PM-driven augmentation of cell surface expression of MHC class II, CD80, and CD86 in both $Nrf2^{+/+}$ and $Nrf2^{-/-}$ DCs while the expression of CD40 by APM-stimulated $Nrf2^{-/-}$ DCs was less sensitive to the effects of NAC, although some minimal inhibition was observed.

Consistent with the observations made above, we found that inflammatory and immunomodulatory cytokines were affected by stimulating DCs with PM. We found that $Nrf2^{-/-}$ DCs secreted constitutively greater levels of IL-12p40, IL-6, IL-10, TNF-$\alpha$, and VEGF than their wt counterparts, and yet DCs lacking *Nrf2* secreted constitutively lower levels of IL-18 as compared with wt DCs. This pattern of cytokine production is consistent with a constitutive and heightened level of DC activation in the absence of functional *Nrf2*. Further, it suggests heightened and relatively unchecked production of ROS as a potential mechanism responsible for enhanced cytokine production.

Activation of DCs from wt mice and those lacking functional *Nrf2* with PM enhanced the production of all cytokines measured, with one notable exception. The secretion of IL-18 was strikingly dampened in $Nrf2^{+/+}$ DCs and enhanced in DCs lacking *Nrf2*. This novel finding suggests that the regulated production of IL-18 is dependent, at least in part, on *Nrf2* activity and free radical production. IL-18 is an important cytokine with roles in septic shock and inflammatory diseases (46). In macrophages, at least, two signals are necessary for the production and secretion of IL-18 (47–49). For IL-18 to be released from the producing cell, a priming and activating signal is required. The priming signal may include a pathogen-associated molecular pattern (such as the classic bacterial danger signal LPS that occupies and transduces a signal via TLR4), but secretion requires cleavage by caspase I. If caspase I is switched off or remains as inactive procaspase I, then IL-18 secretion is dampened (47, 48). It is possible that, in murine DCs expressing *Nrf2*, stimulation with PM is not seen as a "classic danger signal." Alternatively, *Nrf2* (and ROS) may play a role in regulating caspase I activity. Future experiments will be needed to distinguish between these and other possibilities.

In addition, we studied the functional and phenotypic status of highly purified $CD11c^+$ lung myeloid $Nrf2^{+/+}$ and $Nrf2^{-/-}$ DCs upon activation by particulate matter, where we observed remarkable concordance with their bone marrow-derived DCs counterparts. For example, the expression of the costimulatory molecules followed a similar pattern between bone marrow-derived and lung DCs. We noted a consistently dampened expression of CD40 in $Nrf2^{-/-}$ pulmonary DCs relative to their wt counterparts, whereas the expression of both CD80 and particularly CD86 were present at greater levels on $Nrf2^{-/-}$ DCs (Fig. 2*D*). The consistently lowered constitutive expression of CD40 on $Nrf2^{-/-}$ bone marrow as well as lung DCs is of interest because CD40 serves crucial roles in cell-mediated as well as humoral-mediated immunity, particularly in the context of the class switching of Ig to IgE (50, 51). Our data imply an important and as yet unrecognized role for *Nrf2* in regulating the cell surface expression of CD40. However, we know that CD40-CD40L interactions between DCs and T cells, respectively, are required for optimal IgE responses and atopy (52). In human subjects with asthma, CD40 expression is markedly upregulated on a number of different cell types, including macrophages (53), eosinophils (54), and epithelial cells in the conducting airways (55).

In addition, upon activation by particulate matter $Nrf2^{-/-}$ lung (or bone marrow-derived) DCs and their wt counterparts gave augmented levels of expression of CD40, although this was not statistically significant in bone marrow-derived $Nrf2^{-/-}$ DCs (Fig. 2*A*). The synergistic increase in both CD40 expression by $Nrf2^{-/-}$ lung DCs and their ability to promote IL-13 secretion in coculture with naive $CD4^+$ T cells would suggest that Nrf2 normally functions to inhibit proallergic DC phenotypes in vivo. We previously reported that Nrf2-deficient mice develop higher IgE levels in association with more severe allergic airway inflammation after sensitization and challenge with OVA (25). The data contained in this report suggest that this was due at least in part to a greater differentiation of proallergic DCs in the absence of *Nrf2*. It will be important in future studies to define the contribution of Nrf2 in specific cell types to protection from allergen-driven Th2 immune responses in vivo.

Both wt and $Nrf2^{-/-}$ lung DCs promoted an enhanced pro-Th2 cytokine response upon activation by PM, but the magnitude of this response was markedly greater using $Nrf2^{-/-}$ lung DCs. Ratiometric analyses (Fig. 6*C*) revealed that $Nrf2^{-/-}$ lung DCs promoted >5-fold more IL-13 than IFN-$\gamma$ than their wt counterparts and >4-fold greater amounts of IL-13 than IL-12p70 in the DC/$CD4^+$ T cell coculture system. By contrast, $Nrf2^{+/+}$ lung DCs promoted only a 2.8-fold increase in IL-13:IFN-$\gamma$ and a 2.2-fold increase in IL-13:IL-12p70 (Fig. 6*C*), conditions that favor a Th2 bias, but markedly lower than the ratios observed for $Nrf2^{-/-}$ lung DCs.

The observation that $Nrf2^{-/-}$ DCs exhibit an inherent ability to promote pro-Th2 cytokine secretion by responding $CD4^+$ T cells is of considerable interest. The importance of DCs in directing a Th1-type or Th2-type Ag-specific activation of naive T cells in regional draining lymph nodes is now fairly well established and is thought to be largely dependent on the local cytokines secreted by in the immunological synapse with $CD4^+$ T cells as well as other signals (56–58). In the context of allergic Th2-mediated inflammation, effector $CD4^+$ Th2 cells rapidly exit the lymph nodes and migrate to sites of established inflammation whereupon they interact with IgE-bearing tissue DCs to further augment the Th2 cytokine pool, including enhanced production of proallergic cytokines such as IL-5, IL-9, and IL-13 (59–61).

Our data add to a growing body of work indicating that oxidative stress in DCs is an important determinant of the Th1/Th2 balance. For example, it was recently shown that Nrf2 inhibits NF-$\kappa$B-mediated signal transduction, which is critical for the elaboration of IL-12 and TNF-$\alpha$ secretion as well as costimulatory molecules such as CD80, CD86, and CD54 by APCs, including DCs (62). In this elegant study it was further shown that a change

in the intracellular redox status of DCs upon activation by particulates such as diesel exhaust particulates disrupt the normal ability of TLR agonists to mature DCs. This perturbation of DC function was also associated with dampened IFN-γ and augmented IL-10 secretion in Ag-specific T cells (62), which is in keeping with our findings using *Nrf2*$^{-/-}$ DCs, lung myeloid DCs, and ambient PM (Figs. 4 and 6). Our data support the idea that restoring the oxidant/antioxidant balance in DCs may have a therapeutic benefit in Th2-dominant allergic diseases (11, 63).

The effects of NAC on inflammatory cytokine production by wt as well as by *Nrf2*$^{-/-}$ DCs was complex. In resting *Nrf2*$^{+/+}$ wt DCs, NAC suppressed only the secretion of IL-12p40 and TNF and actually enhanced the production of all others, including IL-18 in this model. Thus, in resting DCs with active *Nrf2,* exposing cells to NAC can actually enhance somewhat the release of IL-6, IL-10, IL-18, and VEGF. By contrast, in resting DCs lacking active *Nrf2*, exposing cells to NAC enhanced secretion of only TNF-α and VEGF. The regulation in VEGF secretion between *Nrf2*-expressing DCs and those lacking *Nrf2* was of considerable interest, because we found that *Nrf2*$^{-/-}$ DCs produced markedly more VEGF at baseline than their wt counterparts (Table I).

VEGF is an important mitogen and chemotactic agent that plays diverse roles in tumor growth and survival, wound repair, angiogenesis, microvascular permeability, and asthma (64–66). For example, VEGF dampens IL-12 synthesis and down-modulates the differentiation of CD4$^+$ Th1 cells following their interaction with LPS-matured DCs (67). In addition, VEGF may attenuate the differentiation and maturation of DCs from hematopoietic progenitors (68, 69). Others have shown that VEGF is sensitive to alterations in oxygen tension and to increases in intracellular levels of ROS (70, 71). Indeed, it has been shown that VEGF signaling is associated with the redox state of the cell (68, 69).

In our experiments, VEGF was elevated in *Nrf2*$^{-/-}$ DCs. This would be consistent with the notion that VEGF is linked to the redox state of the cell. We also observed increased expression of HO-1 and other *Nrf2*-regulated antioxidant genes (Fig. 10*C*), in particulate matter-exposed DCs from both *Nrf2*-expressing and *Nrf2*-disrupted mice. Because HO-1 enzymatic activity is an important stimulus for VEGF production (70), one interesting possibility is that *Nrf2* induces VEGF in a HO-1-dependent manner. VEGF may also positively feed back and enhance HO-1 expression in vivo and in vitro (71, 72). This would imply a possible interaction between *Nrf2*-mediated antioxidant signaling and VEGF during DC maturation.

Direct evidence for a pro-oxidative effect of PM on the functional activation of DCs came from studies where we assessed the accumulation of $H_2O_2$ by DCFH-DA assay and quantified ROS synthesis by a luminol-based assay. In these experiments, we found that PM enhanced the accumulation of $H_2O_2$ in *Nrf2*$^{-/-}$ and *Nrf2*$^{-+}$ DCs. DCs lacking expression of *Nrf2* also accumulated more $H_2O_2$ than *Nrf2*$^{+/+}$ DCs, presumably by a compromised ability to detoxify $H_2O_2$. The ambient PM used in our studies is a complex mixture of heavy and transition metals and other particles coalesced around a carbon core (1, 2). The mechanisms by which ambient PM induces oxidative stress include the effects of metals and possibly hydrocarbon and aryl hydrocarbon-containing components. Unlike commonly used diesel exhaust particles that are generated from test engines under experimental conditions, the ambient PM used in our studies reflects "real-world" exposures and is likely derived from multiple sources. Although this adds to the complexity of PM, we feel that this is also a more clinically relevant compound to test in exposure models.

We also looked at the expression of other antioxidant genes to determine the ROS defense systems present as well as the total antioxidative capacity in *Nrf2*$^{-/-}$ as compared with *Nrf2*$^{+/+}$ wt DCs following their exposure to PM. In addition to HO-1, we found that there was a heightened constitutive level of expression of GCLc and HO-1 in resting *Nrf2*$^{+/+}$ DCs as compared with *Nrf2*$^{-/-}$ DCs. It will be interesting in future studies to determine how compromised expression of antioxidant genes in *Nrf2*-deficient DCs leads to enhanced expression of cell surface markers and increased secretion of inflammatory cytokines in response to PM.

Alternative and perhaps complementary explanations for the enhanced constitutive activation of *Nrf2*$^{-/-}$ DCs, particularly following stimulation by PM, may include decreased expression of HO-1 in *Nrf2*$^{-/-}$ DCs relative to their wt counterparts. The mechanisms responsible are complex but may involve the ability of HO-1 to otherwise protect cells against oxidative stress, cellular injury, and inflammation, an activity lacking in *Nrf2*$^{-/-}$ DCs (73). When present in cells expressing Nrf2, the antioxidant enzyme HO-1 metabolizes heme to biliverdin, free divalent iron, and carbon monoxide (74). The relevance of this is that biliverdin is further metabolized to bilirubin and both are powerful antioxidant and immunosuppressive proteins (75).

In summary, *Nrf2*-disrupted DCs exhibit a heightened and constitutively proinflammatory state. These observations indicate an important role for *Nrf2* in gauging an appropriate pattern of inflammatory activation of DCs in response to danger signals such as environmental particulate matter or other allergens. Disruption of the *Nrf2* gene may potentially enhance host susceptibility to various allergic or infectious diseases, although this awaits formal demonstration.

## Acknowledgments

We thank Dr. Peyton Eggleston and his team at the Johns Hopkins National Institute of Environmental Health Sciences Center for Childhood Asthma in the Urban Environment, Baltimore, MD for their enthusiastic support and Dr. John McDyer (Johns Hopkins University, Baltimore, MD) for providing trimeric CD40L. We also thank Dr. David Topham, Department of Immunology and Microbiology, University of Rochester, Rochester, NY for kindly providing the male OT-II mice used in these studies.

## Disclosures

The authors have no financial conflict of interest.

## References

1. Walters, D. M., P. N. Breysse, B. Schofield, and M. Wills-Karp. 2002. Complement factor 3 mediates particulate matter-induced airway hyperresponsiveness. *Am. J. Respir. Cell Mol. Biol.* 27: 413–418.
2. Williams, M. A., M. Porter, J. Guo, J. Roman, D. Williams, P. N. Breysse, and S. N. Georas. 2007. Ambient particulate matter directs non-classical immunological activation of dendritic cells and promotes Th2-like polarization. *J. Allergy Clin. Immunol.* 119: 488–497.
3. Saxon, A., and D. Diaz-Sanchez. 2005. Air pollution and allergy: you are what you breathe. *Nat. Immunol.* 6: 223–226.
4. Laden, F., J. Schwartz, F. E. Speizer, and D. W. Dockery. 2006. Reduction in fine particulate air pollution and mortality: extended follow-up of the Harvard Six Cities Study. *Am. J. Respir. Crit. Care Med.* 173: 667–672.
5. Dominici, F., A. McDermott, M. Daniels, S. L. Zeger, and J. M. Samet. 2005. Revised analyses of the National Morbidity, Mortality, and Air Pollution Study: mortality among residents of 90 cities. *J. Toxicol. Environ. Health A* 68: 1071–1092.
6. Mellman, I., and R. M. Steinman. 2001. Dendritic cells: specialized and regulated antigen processing machines. *Cell* 106: 255–258.
7. Hammad, H., and B. N. Lambrecht. 2007. Lung dendritic cell migration. *Adv. Immunol.* 93: 265–278.
8. Langenkamp, A., M. Messi, A. Lanzavecchia, and F. Sallusto. 2000. Kinetics of dendritic cell activation: impact on priming of TH1, TH2, and nonpolarized T cells. *Nat. Immunol.* 1: 311–316.
9. Vermaelen, K., and R. Pauwels. 2005. Pulmonary dendritic cells. *Am. J. Respir. Crit. Care Med.* 172: 530–551.
10. Bleck, B., D. B. Tse, I. Jaspers, M. A. Curotto de Lafaille, and J. Reibman. 2006. Diesel exhaust particle-exposed human bronchial epithelial cells induce dendritic cell maturation. *J. Immunol.* 176: 7431–7437.
11. Finkelman, F. D., M. Yang, T. Orekhova, E. Clyne, J. Bernstein, M. Whitekus, D. Diaz-Sanchez, and S. C. Morris. 2004. Diesel exhaust particles suppress in

vivo IFN-γ production by inhibiting cytokine effects on NK and NKT cells. *J. Immunol.* 172: 3808–3813.
12. Blank, F., B. Rothen-Rutishauser, and P. Gehr. 2007. Dendritic cells and macrophages form a transepithelial network against foreign particulate antigens. *Am. J. Respir. Cell Mol. Biol.* 36: 669–677.
13. Tse, H. M., M. J. Milton, S. Schreiner, J. L. Profozich, M. Trucco, and J. D. Piganelli. 2007. Disruption of innate-mediated proinflammatory cytokine and reactive oxygen species third signal leads to antigen-specific hyporesponsiveness. *J. Immunol.* 178: 908–917.
14. Kuppner, M. C., A. Scharner, V. Milani, C. Von Hesler, K. E. Tschop, O. Heinz, and R. D. Issels. 2003. Fosfamide impairs the allostimulatory capacity of human dendritic cells by intracellular glutathione depletion. *Blood* 102: 3668–3674.
15. Murata, Y., T. Ohteki, S. Koyasu, and J. Hamuro. 2002. IFN-γ and proinflammatory cytokine production by antigen-presenting cells is dictated by intracellular thiol redox status regulated by oxygen tension. *Eur. J. Immunol.* 32: 2866–2873.
16. Mizuashi, M., T. Ohtani, S. Nakagawa, and S. Aiba. 2005. Redox imbalance induced by contact sensitizers triggers the maturation of dendritic cells. *J. Invest. Dermatol.* 124: 579–586.
17. Matsue, H., D. Edelbaum, D. Shalhevet, N. Mizumoto, C. Yang, M. E. Mummert, J. Oeda, H. Masayasu, and A. Takashima. 2003. Generation and function of reactive oxygen species in dendritic cells during antigen presentation. *J. Immunol.* 171: 3010–3018.
18. Alderman, C. J., S. Shah, J. C. Foreman, B. Chain, and D. R. Katz. 2002. The role of advanced oxidation protein products in regulation of dendritic cell function. *Free Radical Biol. Med.* 32: 377–385.
19. Kim, H. J., B. Barajas, R. Chun-Fai Chan, and A. E. Nel. 2007. Glutathione depletion inhibits dendritic cell maturation and delayed-type hypersensitivity: implications for systemic disease and immunosenescence. *J. Allergy Clin. Immunol.* 119: 1225–1233.
20. Gilston, V., M. A. Williams, A. C. Newland, and P. G. Winyard. 2001. Hydrogen peroxide and tumour necrosis factor-α induce NF-κB-DNA binding in primary human T lymphocytes in addition to T cell lines. *Free Radical Res.* 35: 681–691.
21. Rangasamy, T., C. Y. Cho, R. K. Thimmulappa, L. Zhen, S. S. Srisuma, T. W. Kensler, M. Yamamoto, I. Petrache, R. M. Tuder, and S. Biswal. 2004. Genetic ablation of Nrf2 enhances susceptibility to cigarette smoke-induced emphysema in mice. *J. Clin. Invest.* 114: 1248–1259.
22. Li, N., M. I. Venkatesan, A. Miguel, R. Kaplan, C. Gujuluva, J. Alam, and A. Nel. 2000. Induction of heme oxygenase-1 expression in macrophages by diesel exhaust particle chemicals and quinones via the antioxidant-responsive element. *J. Immunol.* 165: 3393–3401.
23. Li, N., J. Alam, M. I. Venkatesan, A. Eiguren-Fernandez, D. Schmitz, E. Di Stefano, N. Slaughter, E. Killeen, X. Wang, A. Huang, et al. 2004. Nrf2 is a key transcription factor that regulates antioxidant defense in macrophages and epithelial cells: protecting against the proinflammatory and oxidizing effects of diesel exhaust chemicals. *J. Immunol.* 173: 3467–3481.
24. Kweon, M. H., V. M. Adhami, J. S. Lee, and H. Mukhtar. 2006. Constitutive overexpression of Nrf2-dependent heme oxygenase-1 in A549 cells contributes to resistance to apoptosis induced by epigallocatechin 3-gallate. *J. Biol. Chem.* 281: 33761–33772.
25. Rangasamy, T., J. Guo, W. A. Mitzner, J. Roman, A. Singh, A. D. Fryer, M. Yamamoto, T. W. Kensler, R. M. Tuder, S. N. Georas, and S. Biswal. 2005. Disruption of Nrf2 enhances susceptibility to severe airway inflammation and asthma in mice. *J. Exp. Med.* 202: 47–59.
26. Reddy, N. M., S. R. Kleeberger, H. Y. Cho, M. Yamamoto, T. W. Kensler, S. Biswal, and S. P. Reddy. 2007. Deficiency in Nrf2-GSH signaling impairs type II cell growth and enhances sensitivity to oxidants. *Am. J. Respir. Cell Mol. Biol.* 37: 3–8.
27. Zhang, D. D. 2006. Mechanistic studies of the Nrf2-Keap1 signaling pathway. *Drug Metab. Rev.* 38: 769–789.
28. Kensler, T. W., N. Wakabayashi, and S. Biswal. 2007. Cell survival responses to environmental stresses via the Keap1-Nrf2-ARE pathway. *Annu. Rev. Pharmacol. Toxicol.* 47: 89–116.
29. Thimmulappa, R. K., H. Lee, T. Rangasamy, S. P. Reddy, M. Yamamoto, T. W. Kensler, and S. Biswal. 2006. Nrf2 is a critical regulator of the innate immune response and survival during experimental sepsis. *J. Clin. Invest.* 116: 984–995.
30. Itoh, K., T. Chiba, S. Takahashi, T. Ishii, K. Igarashi, Y. Katoh, T. Oyake, N. Hayashi, K. Satoh, I. Hatayama, et al. 1997. An Nrf2/small Maf heterodimer mediates the induction of phase II detoxifying enzyme genes through antioxidant response elements. *Biochem. Biophys. Res. Commun.* 236: 313–322.
31. Williams, M. A., R. S. Trout, and S. A. Spector. 2002. HIV-1 gp120 modulates the immunological function and expression of accessory and co-stimulatory molecules of monocyte-derived dendritic cells. *J. Hematother. Stem Cell Res.* 11: 829–847.
32. Williams, M. A., S. M. Kelsey, P. W. Collins, C. N. Gutteridge, and A. C. Newland. 1995. Administration of rHuGM-CSF activates monocyte reactive oxygen species secretion and adhesion molecule expression in vivo in patients following high-dose chemotherapy. *Br. J. Haematol.* 90: 31–40.
33. Williams, M. A., S. A. White, J. J. Miller, C. Toner, S. Withington, A. C. Newland, and S. M. Kelsey. 1998. Granulocyte-macrophage colony-stimulating factor induces activation and restores respiratory burst activity in monocytes from septic patients. *J. Infect. Dis.* 177: 107–115.
34. Trush, M. A., and K. Van Dyke. 1978. Effect of promethazine on human polymorphonuclear chemiluminescence. *Pharmacology* 16: 314–320.
35. Berry, M., C. Brightling, I. Pavord, and A. Wardlaw. 2007. TNF-α in asthma. *Curr. Opin. Pharmacol.* 7: 279–282.
36. Nakae, S., C. Lunderius, L. H. Ho, B. Schäfer, M. Tsai, and S. J. Galli. 2007. TNF can contribute to multiple features of ovalbumin-induced allergic inflammation of the airways in mice. *J. Allergy Clin. Immunol.* 119: 680–686.
37. Meyts, I., P. W. Hellings, G. Hens, B. M. Vanaudenaerde, B. Verbinnen, H. Heremans, P. Matthys, D. M. Bullens, L. Overbergh, C. Mathieu, et al. 2006. IL-12 contributes to allergen-induced airway inflammation in experimental asthma. *J. Immunol.* 177: 6460–6470.
38. Cooper, A. M., and S. A. Khader. 2007. IL-12p40: an inherently agonistic cytokine. *Trends Immunol.* 28: 33–38.
39. McKinley, L., J. Kim, G. L. Bolgos, J. Siddiqui, and D. G. Remick. 2005. CXC chemokines modulate IgE secretion and pulmonary inflammation in a model of allergic asthma. *Cytokine* 32: 178–185.
40. Vargaftig, B. B., and M. Singer. 2003. Leukotrienes, IL-13, and chemokines cooperate to induce BHR and mucus in allergic mouse lungs. *Am. J. Physiol.* 284: L260–L269.
41. Chauveau, C., S. Remy, P. J. Royer, M. Hill, S. Tanguy-Royer, F. X. Hubert, L. Tesson, R. Brion, G. Beriou, M. Gregoire, et al. 2005. Heme oxygenase-1 expression inhibits dendritic cell maturation and proinflammatory function but conserves IL-10 expression. *Blood* 106: 1694–1702.
42. Ohtani, T., S. Nakagawa, M. Kurosawa, M. Mizuashi, M. Ozawa, and S. Aiba. 2005. Cellular basis of the role of diesel exhaust particles in inducing Th2-dominant response. *J. Immunol.* 174: 2412–2419.
43. Kantengwa, S., L. Jornot, C. Devenoges, and L. P. Nicod. 2003. Superoxide anions induce the maturation of human dendritic cells. *Am. J. Respir. Crit. Care Med.* 167: 431–437.
44. Verhasselt, V., W. Vanden Berghe, N. Vanderheyde, F. Willems, G. Haegeman, and M. Goldman. 1999. *N*-acetyl-L-cysteine inhibits primary human T cell responses at the dendritic cell level: association with NF-κB inhibition. *J. Immunol.* 162: 2569–2574.
45. Rutault, K., C. Alderman, B. M. Chain, and D. R. Katz. 1999. Reactive oxygen species activate human peripheral blood dendritic cells. *Free Radical Biol. Med.* 26: 232–238.
46. Boraschi, D., and C. A. Dinarello. CA. IL-18 in autoimmunity. 2006. *Eur. Cytokine Network* 17: 224–252.
47. Lich, J. D., J. C. Arthur, and J. P. Ting. 2006. Cryopyrin: in from the cold. *Immunity* 24: 241–243.
48. Meylan, E., J. Tschopp, and M. Karin. 2006. Intracellular pattern recognition receptors in the host response. *Nature* 442: 39–44.
49. Kang, M. J., R. J. Homer, A. Gallo, C. G. Lee, K. A. Crothers, S. J. Cho, C. Rochester, H. Cain, G. Chupp, H. J. Yoo, and J. A. Elias. 2007. IL-18 is induced and IL-18 receptor α plays a critical role in the pathogenesis of cigarette smoke-induced pulmonary emphysema and inflammation. *J. Immunol.* 178: 1948–1459.
50. Looney, R. J., D. Pudia, and S. I. Rosenfeld. 1994. Cytokine production by mite-specific T cells from donors with mild atopic disease. *J. Allergy Clin. Immunol.* 93: 476–483.
51. Jabara, H. H., S. M. Fu, R. S. Geha, and D. Vercelli. 1990. CD40 and IgE: synergism between anti-CD40 monoclonal antibody and interleukin 4 in the induction of IgE synthesis by highly purified human B cells. *J. Exp. Med.* 172: 1861–1864.
52. Kroczek, R., and E. Hamelmann. 2005. T-cell costimulatory molecules: optimal targets for the treatment of allergic airway disease with monoclonal antibodies. *J. Allergy Clin. Immunol.* 116: 906–909.
53. Tang, C., C. Ward, D. Reid, R. Bish, P. M. O'Byrne, and E. H. Walters. 2001. Normally suppressing CD40 coregulatory signals delivered by airway macrophages to TH2 lymphocytes are defective in patients with atopic asthma. *J. Allergy Clin. Immunol.* 107: 863–870.
54. Bureau, F., G. Seumois, F. Jaspar, A. Vanderplasschen, B. Detry, P. Pastoret, R. Louis, and P. Lekeux. 2002. CD40 engagement enhances eosinophil survival through induction of cellular inhibitor of apoptosis protein 2 expression: possible involvement in allergic inflammation. *J. Allergy Clin. Immunol.* 110: 443–449.
55. Propst, S. M., R. Denson, E. Rothstein, K. Estell, and L. M. Schwiebert. 2000. Proinflammatory and Th2-derived cytokines modulate CD40-mediated expression of inflammatory mediators in airway epithelia: implications for the role of epithelial CD40 in airway inflammation. *J. Immunol.* 165: 2214–2221.
56. Eisenbarth, S. C., D. A. Piggott, and K. Bottomly. 2003. The master regulators of allergic inflammation: dendritic cells in Th2 sensitization. *Curr. Opin. Immunol.* 15: 620–626.
57. O'Garra, A., and N. Arai. 2000. The molecular basis of T helper 1 and T helper 2 cell differentiation. *Trends Cell Biol.* 10: 542–550.
58. Moser, M., and K. M. Murphy. 2000. Dendritic cell regulation of TH1-TH2 development. *Nat. Immunol.* 1: 199–205.
59. Thepen, T., C. McMenamin, B. Girn, G. Kraal, and P. G. Holt. 1992. Regulation of IgE production in pre-sensitized animals: in vivo elimination of alveolar macrophages preferentially increases IgE responses to inhaled allergen. *Clin. Exp. Allergy* 22: 1107–1114.
60. Van Rijt, L. S., S. Jung, A. Kleinjan, N. Vos, M. Willart, C. Duez, H. C. Hoogsteden, and B. N. Lambrecht. 2005. In vivo depletion of lung $CD11c^+$ dendritic cells during allergen challenge abrogates the characteristic features of asthma. *J. Exp. Med.* 201: 981–991.
61. Lambrecht, B. N., M. De Veerman, A. J. Coyle, J. C. Gutierrez-Ramos, K. Thielemans, and R. A. Pauwels. 2000. Myeloid dendritic cells induce Th2 responses to inhaled antigen, leading to eosinophilic airway inflammation. *J. Clin. Invest.* 106: 551–559.

62. Chan, R. C., M. Wang, N. Li, Y. Yanagawa, K. Onoé, J. J. Lee, and A. E. Nel. 2006. Pro-oxidative diesel exhaust particle chemicals inhibit LPS-induced dendritic cell responses involved in T-helper differentiation. *J. Allergy Clin. Immunol.* 118: 455–465.
63. Kidd, P. 2003. Th1/Th2 balance: the hypothesis, its limitations, and implications for health and disease. *Altern. Med. Rev.* 8: 223–246.
64. Cross, M. J., J. Dixelius, T. Matsumoto, and L. Claesson-Welsh. 2003. VEGF-receptor signal transduction. *Trends Biochem. Sci.* 28: 488–494.
65. Alavi, A., J. D. Hood, R. Frausto, D. G. Stupack, and D. A. Cheresh. 2003. Role of Raf in vascular protection from distinct apoptotic stimuli. *Science* 301: 94–96.
66. Lee, C. G., H. Link, P. Baluk, R. J. Homer, S. Chapoval, V. Bhandari, M. J. Kang, L. Cohn, Y. K. Kim, D. M. McDonald, and J. A. Elias. 2004. Vascular endothelial growth factor (VEGF) induces remodeling and enhances TH2-mediated sensitization and inflammation in the lung. *Nat. Med.* 10: 1095–1103.
67. Takahashi, A., K. Kono, F. Ichihara, H. Sugai, H. Fujii, and Y. Matsumoto. 2004. Vascular endothelial growth factor inhibits maturation of dendritic cells induced by lipopolysaccharide, but not by proinflammatory cytokines. *Cancer Immunol. Immunother.* 53: 543–550.
68. Oyama, T., S. Ran, T. Ishida, S. Nadaf, L. Kerr, D. P. Carbone, and D. I. Gabrilovich. 1998. Vascular endothelial growth factor affects dendritic cell maturation through the inhibition of nuclear factor-κB activation in hemopoietic progenitor cells. *J. Immunol.* 160: 1224–1232.
69. Kang, H. K., J. S. Park, S. K. Kim, B. H. Choi, T. N. Pham, X. W. Zhu, D. Cho, J. H. Nam, Y. J. Kim, J. H. Rhee, et al. 2006. Down-regulation of cellular vascular endothelial growth factor levels induces differentiation of leukemic cells to functional leukemic-dendritic cells in acute myeloid leukemia. *Leuk. Lymphoma* 47: 2224–2233.
70. Angermayr, B., M. Mejias, J. Gracia-Sancho, J. C. Garcia-Pagan, J. Bosch, and M. Fernandez. 2006. Heme oxygenase attenuates oxidative stress and inflammation, and increases VEGF expression in portal hypertensive rats. *J. Hepatol.* 44: 1033–1039.
71. Fernandez, M., and H. L. Bonkovsky. 2003. Vascular endothelial growth factor increases heme oxygenase-1 protein expression in the chick embryo chorioallantoic membrane. *Br. J. Pharmacol.* 139: 634–640.
72. Bussolati, B., A. Ahmed, H. Pemberton, R. C. Landis, F. Di Carlo, D. O. Haskard, and J. C. Mason. 2004. Bifunctional role for VEGF-induced heme oxygenase-1 in vivo: induction of angiogenesis and inhibition of leukocytic infiltration. *Blood* 103: 761–766.
73. Hsieh, C. S., S. E. Macatonia, C. S. Tripp, S. F. Wolf, A. O'Garra, and K. M. Murphy. 1993. Development of TH1 $CD4^+$ T cells through IL-12 produced by *Listeria*-induced macrophages. *Science* 260: 547–549.
74. Otterbein, L. E., and A. M. Choi. 2000. Heme oxygenase: colors of defense against cellular stress. *Am. J. Physiol.* 279: L1029–L1037.
75. Yamashita, K., R. Ollinger, J. McDaid, H. Sakahama, H. Wang, S. Tyagi, E. Csizmadia, N. R. Smith, M. P. Soares, and F. H. Bach. 2006. Heme oxygenase-1 is essential for and promotes tolerance to transplanted organs. *FASEB J.* 20: 776–778.